QCD PHYSICS OPPORTUNITIES IN LOW-ENERGY ELECTRON-POSITRON ANNIHILATION*

Stanley J. Brodsky
Stanford Linear Accelerator Center
Stanford University, Stanford, California 94309
E-mail: sjbth@slac.stanford.edu

QCD PHYSICS OPPORTUNITIES IN LOW-ENERGY ELECTRON-POSITRON ANNIHILATION[*]

Stanley J. Brodsky[†], SLAC, Stanford, CA 94305, USA

Abstract

I survey a number of interesting tests of quantum chromodynamics at the amplitude level which can be carried out in electron-positron annihilation and in photon-photon collisions at low energy. Some of the tests require e^+e^- center of mass energy as small as $\sqrt{s} = 2$ GeV. Other tests which involve a spectrum of energies can be carried out advantageously at high energy facilities using the radiative return method. These include measurements of fundamental processes such as timelike form factors and transition amplitudes, timelike Compton scattering, timelike photon to meson transition amplitudes, and two-photon exclusive processes. Many of these reactions test basic principles of QCD such as hadronization at the amplitude level, factorization, and hadron helicity conservation, tools also used in the analysis of exclusive B and D decays. Measurements of the final-state polarization in hadron pair production determine the relative phase of the timelike form factors and thus strongly discriminate between analytic forms of models which fit the form factors in the spacelike region. The role of two-photon exchange amplitudes can be tested using the charge asymmetry of the $e^+e^- \to B\overline{B}$ processes. These tests can help resolve the discrepancy between the Jefferson laboratory measurements of the ratio of G_E and G_M proton form factors using the polarization transfer method versus measurements using the traditional Rosenbluth method. Precision measurements of the electron-positron annihilation cross section can test the generalized Crewther relation and determine whether the effective couplings defined from physical measurements show infrared fixed-point and near conformal behavior. I also discuss a number of tests of novel QCD phenomena accessible in e^+e^- annihilation, including near-threshold reactions, the production of baryonium, gluonium states, and pentaquarks.

INTRODUCTION

Quantum Chromodynamics has been very well tested at high energies, particularly in inclusive reactions involving large momentum transfers much higher than the QCD scale Λ_{QCD}. Tests of QCD at low energies are much more challenging, since they require an understanding of nonperturbative elements of the theory, including the behavior of the QCD coupling at low momentum transfers, the fundamental features of hadron wavefunctions, and the fundamental color coherence of QCD interactions.

In this talk I will survey a number of tests of QCD which test fundamental issues of hadron physics at the amplitude level. These include measurements of fundamental processes such as timelike form factors and transition amplitudes, timelike Compton scattering, timelike photon to meson transition amplitudes, and two-photon exclusive processes. Many of these reactions test basic principles of QCD such as factorization and hadron helicity conservation, tools also used in the analysis of exclusive B and D decays. Electron-positron annihilation can determine whether the effective couplings defined from physical measurements show infrared fixed-point and near-conformal behavior. I also discuss a number of tests of novel QCD phenomena accessible in e^+e^- annihilation, including near-threshold reactions, the production of baryonium, gluonium states, and pentaquarks.

There has recently been a number of experimental surprises in QCD spectroscopy and heavy quark production which show the importance of detailed measurements in electron-positron collisions. These include:

1. The cross section measured at Belle [1] for double-charmonium production $e^+e^- \to J/\psi\eta_c$ and $J/\psi DX$ is an order of magnitude larger than predicted [2], It is important to see whether this anomaly also holds for analogous channels involving strangeness: $e^+e^- \to \phi\eta$ and ϕKX.

2. The evidence for the predicted gluonic bound states gg, ggg, $q\bar{q}g$ spectroscopy of QCD is still not conclusive. The subprocesses $e^+e^- \to c\bar{c}gg$ and $e^+e^- \to c\bar{c}c\bar{c}$ have comparable rates, suggesting a large role for the production of associated charmonium plus gluonic states. See Fig. 1. Fred Goldhaber, Jungil Lee and I have recently calculated the cross section for $e^+e^- \to H\mathcal{G}_{J=0,2}$ using perturbative QCD factorization [3]. We find that $\gamma^* \to J/\psi\mathcal{G}_0$ production dominates over that of $J/\psi\mathcal{G}_2$, and show how the angular distribution of the final state can be used to determine the angular momentum J and projection J_z of the glueball; only $J_z = \pm 2$ tensor states are produced by the perturbative QCD mechanism at leading twist. The rate for $e^+e^- \to J/\psi\mathcal{G}_0$ production could be comparable to the corresponding nonrelativistic QCD (NRQCD) prediction for $e^+e^- \to J/\psi\eta_c$ without exceeding the known bound from radiative Υ decay. Another interesting glueball search process is the missing mass spectrum in $e^+e^- \to \phi X$.

3. New signals for baryonium resonances just below threshold in $p\bar{p} \to e^+e^-$ (odd charge conjugation) and $J/\psi \to (p\bar{p})\gamma$ (even charge conjugation) have been reported [4, 5, 6], but not in $J/\psi \to (p\bar{p})\pi^0$ (odd charge
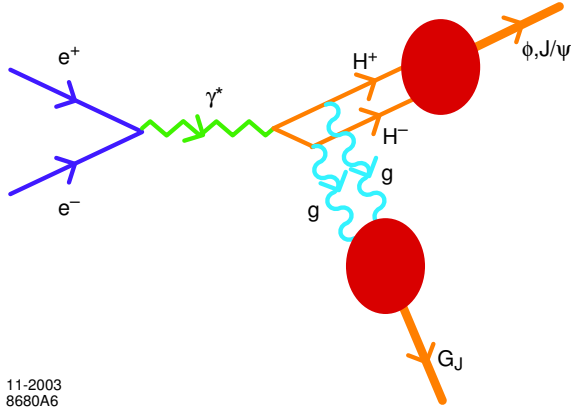

[†] sjbth@slac.stanford.edu

Figure 1: Illustration of QCD mechanism for the exclusive production of quarkonium and gluonium in electron-positron collisions.

Figure 2: Mechanisms for producing baryon pairs and pentaquarks

conjugation). A strong threshold enhancement is also observed in $p\bar{p} \to e^+e^-$ [7]. These near-threshold states may reflect the binding of qqq or qq systems, the QCD van der Waals interaction [8, 9], quark interchange covalent bonds, or attractive meson exchange interactions analogous to the nuclear potential [10, 11]. It is important to test this phenomenon not only in baryon production near threshold $e^+e^- \to B\overline{B}$ and $\gamma\gamma \to B\overline{B}$, but also for any hadron-pair threshold. It is also interesting to study the formation of Coulomb-bound atomic states such as $\mu^+\mu^-$ and $\tau^+\tau^-$.

4. The recent discovery [12, 13, 14, 15] of a pentaquark state $\Theta^+(uddu\bar{s})$ indicates that the spectroscopy of QCD is much richer than previously thought [16, 17, 18, 19, 20] These states could be produced and analyzed in exclusive reactions such as $e^+e^- \to \Theta^+(uudd\bar{s})\Theta^-(\overline{uudd}s)$ and $e^+e^- \to \Theta^+(uudd\bar{s})K^-(\bar{u}s)\bar{n}(\overline{udd})$ or $\Theta^+\overline{K}^0\bar{p}$. See Fig. 2. These types or reactions can give decisive information on the quantum numbers of the new states. The form factor for timelike pentaquark pair production is predicted to falloff as s^{-4} according to dimensional counting rules.

5. The transition form factor for $ep \to e\Delta^+$ falls anomalously fast at high spacelike q^2 compared to other $ep \to eN^*$ form factors [21]. Is this due to a special characteristic of Δ substructure? For example, if the Δ^+ is dominantly a pentaquark $uuu\bar{d}$ state, then the timelike $e^+e^- \to \bar{p}\Delta^+$ transition form factor will fall as s^{-3} compared to the canonical s^{-2} QCD fall-off for timelike baryon pair form factors.

6. The phenomenology of J/ψ decays is still puzzling [22]. For example, the decay $J/\psi \to \rho\pi$ is the largest two-body decay channel for the J/ψ even though the decay of the J/ψ with $J^z = \pm 1$ to pseudoscalar vector channels is forbidden by hadron helicity conservation [23], which follows from QCD factorization and the chirality conservation of QCD interactions. In contrast, the ψ' has not been observed to decay to $\rho\pi$. As discussed below, an intriguing solution of this puzzle is the presence of intrinsic heavy
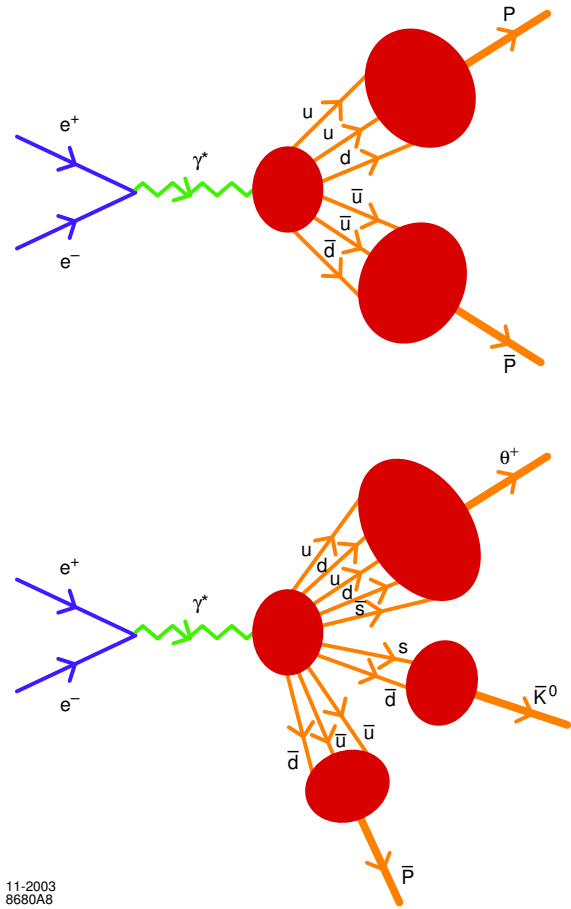
quark Fock states in the light hadrons [24]. It is important to verify whether hadron-helicity conservation is observed in the continuum production of meson pairs; *e.g.*, $e^+e^- \to \rho\pi$ should be strongly suppressed.

7. The form factors of hadrons as measured in both the spacelike and timelike domains provide fundamental information on the structure and internal dynamics of hadrons. Recent measurements [25] of the electron-to-proton polarization transfer in $\vec{e}^- p \to e^- \vec{p}$ scattering at Jefferson Laboratory show that the ratio of spacelike Sachs form factors [26] $G_E^p(q^2)/G_M^p(q^2)$ is monotonically decreasing with increasing $Q^2 = -q^2$, in strong contradiction with the G_E/G_M scaling determined by the traditional Rosenbluth separation method. The Rosenbluth method may in fact not be reliable, perhaps because of its sensitivity to uncertain radiative corrections, including two-photon exchange amplitudes [27]. The polarization transfer method [25, 28] is relatively insensitive to such corrections.

The same data which indicate that G_E for protons falls faster than G_M at large spacelike Q^2 require in turn that F_2/F_1 falls more slowly than $1/Q^2$. The conventional expectation from dimensional counting rules [29] and perturbative QCD [30] is that the Dirac form factor F_1 should fall

with a nominal power $1/Q^4$, and the ratio of the Pauli and Dirac form factors, F_2/F_1, should fall like $1/Q^2$, at high momentum transfers. The Dirac form factor agrees with this expectation in the range Q^2 from a few GeV^2 to the data limit of 31 GeV^2. However, the Pauli/Dirac ratio is not observed to fall with the nominal expected power, and the experimenters themselves have noted that the data is well fit by $F_2/F_1 \propto 1/Q$ in the momentum transfer range 2 to 5.6 GeV^2.

The new Jefferson Laboratory results make it critical to carefully identify and separate the timelike G_E and G_M form factors by measuring the center-of-mass angular distribution and by measuring the polarization of the proton in baryon pair $e^+e^- \to B\overline{B}$ reactions. Polarization measurements can determine phase structure of the timelike form factors and thus provide a remarkable window into QCD at the amplitude level [31]. The role of two-photon exchange amplitudes can be tested using the charge asymmetry of the $e^+e^- \to B\overline{B}$ processes. The advent of high luminosity e^+e^- colliders at Frascati and elsewhere provide the opportunity to make such measurements, both directly and via radiative return.

The advent of electron-positron colliders of high luminosity thus can open up a new range of sensitive tests of QCD. The following sections give an introduction to the theory of a number of e^+e^- collider topics including hard exclusive processes such as timelike Compton scattering, timelike photon-to-pion transition amplitudes, two-photon exclusive processes and single-spin polarization asymmetries. Many of these topics test the main tools used in the analysis of exclusive B and D decays and thus are highly relevant to progress in that field.

Some of the tests discussed here require e^+e^- center of mass energy as small as $\sqrt{s} = 2$ GeV. Other tests which involve a spectrum of energies can be carried out advantageously at high energy facilities using initial-state radiation [32, 33, 34]. See Fig. 3. Recent results from KLOE and BaBar are given in [32, 33, 34]. The radiation of a hard photon from the initial-state electron or the positron allows one to measure the annihilation cross section at a lower energy $s(1-x)$. The basic formula is:

$$\frac{d\sigma(s,x)}{dx} = W(s,x)\sigma[s(1-x)] \qquad (1)$$

where in Born approximation

$$W(s,x) = \frac{2\alpha}{\pi x}(2\ln\sqrt{\frac{s}{m_e}} - 1)(1 - x + \frac{x^2}{2}) \qquad (2)$$

Although the effective luminosity using ISR is reduced by the probability for radiation, this is compensated by the fact that one measures the entire spectrum at one setting of s. The hard photons are primarily radiated along the initial lepton direction. Half of the radiative cross section occurs at $\theta \leq \sqrt{\frac{m_e}{E_e}}$. If the photon is radiated at large angles, then one can test for single spin asymmetries relative to the normal $\vec{n} = \vec{p}_{e^+} \times \vec{p}_{e^-}$ to the annihilation plane.
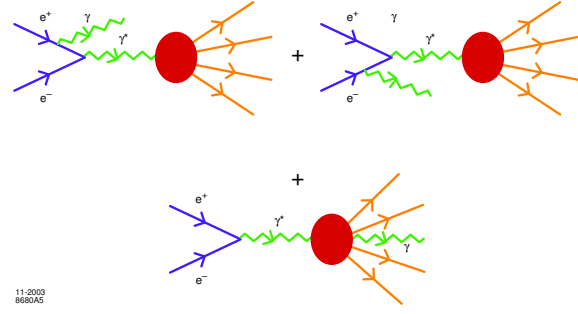

Figure 3: Illustration of initial state radiation in electron-positron collisions. The contribution where the photon is emitted from the hadron currents causes charge and spin asymmetries.

In radiative inclusive reactions, $e^+e^- \to q\bar{q}\gamma$, the interference of initial and final state radiation produces jet charge asymmetries which measure the cube of the quark charge e_q^3. [35, 36] The hadron charge asymmetry in semi-inclusive reactions $e^+e^- \to H^\pm\gamma X$ determines interesting odd charge-conjugation fragmentation functions [35]. In the case of exclusive reactions, one can use the hadron charge asymmetry to measure the interference of the timelike Compton amplitude $e^+e^- \to \gamma^* \to H^+H^-\gamma$ with the timelike form factor appearing in the initial state radiation amplitude $e^+e^- \to \gamma^*\gamma \to H^+H^-\gamma$. This remarkable physics potential is discussed in more detail below. The corresponding formulae for lepton charge asymmetries in $e^+e^- \to \ell\bar{\ell}\gamma$ are given in Ref. [35]

EXCLUSIVE PROCESSES IN QCD

Hard hadronic exclusive processes such as timelike annihilation $e^+e^- \to H\overline{H}$ and $\gamma\gamma \to H\overline{H}$ are at the forefront of low energy QCD studies, particularly because of their role in the interpretation of exclusive hadronic B decays, processes which are essential for determining the CKM phases and the physics of CP violation. Perturbative QCD and its factorization properties at high momentum transfer provide an essential guide to the phenomenology of exclusive amplitudes at large momentum transfer—the leading power fall-off of form factors and fixed-angle cross sections, the dominant helicity structures, and their color transparency properties. The perturbative QCD predictions for two photon reactions can be compared with a phenomenological successful model based on the handbag approximation [37].

A primary issue is the nature and shapes of hadron light-front wavefunctions, the amplitudes which interpolate between hadrons and their quark and gluon degrees of freedom. This is particular important for B physics since the calculation of exclusive hadronic B are computed from the convolution of hadron wavefunctions and distribution amplitudes. For example, the decay amplitude for $B \to \ell\bar{\nu}\pi$ is exactly given by the overlap of B and π light-front wave-

functions. Furthermore the phase structure of hadronic amplitudes and the effects of color transparency are directly relevant to the analysis of phase structure of B decays.

There has been considerable progress analyzing exclusive and diffractive reactions at large momentum transfer from first principles in QCD. Rigorous statements can be made on the basis of asymptotic freedom and factorization theorems which separate the underlying hard quark and gluon subprocess amplitude from the nonperturbative physics of the hadronic wavefunctions. The leading-power contribution to exclusive hadronic amplitudes such as quarkonium decay, heavy hadron decay, and scattering amplitudes involving large momentum transfer can usually be factorized as a convolution of distribution amplitudes $\phi_H(x_i, \Lambda)$ and hard-scattering quark/gluon scattering amplitudes T_H integrated over the light-cone momentum fractions of the valence quarks [38]:

$$\mathcal{M}_{\text{Hadron}} \;=\; \int \prod \phi_H^{(\Lambda)}(x_i, \lambda_i)\, T_H^{(\Lambda)} dx_i \,. \quad (3)$$

Here $T_H^{(\Lambda)}$ is the underlying quark-gluon scattering amplitude subprocess in which each incident and final hadron is replaced by valence quarks with collinear momenta $k_i^+ = x_i p_H^+$, $\vec{k}_{\perp i} = x_i \vec{p}_{\perp H}$. The invariant mass of all intermediate states in T_H is evaluated above the separation scale $\mathcal{M}_n^2 > \Lambda^2$. The essential part of the hadronic wavefunction is the distribution amplitude [38], defined as the integral over transverse momenta of the valence (lowest particle number) Fock wavefunction; *e.g.* for the pion

$$\phi_\pi(x_i, Q) \equiv \int d^2 k_\perp \, \psi_{q\bar{q}/\pi}^{(Q)}(x_i, \vec{k}_{\perp i}, \lambda) \quad (4)$$

where the separation scale Λ can be taken to be order of the characteristic momentum transfer Q in the process. It should be emphasized that the hard scattering amplitude T_H is evaluated in the QCD perturbative domain where the propagator virtualities are above the separation scale. The leading power fall-off of the hard-scattering amplitude as given by dimensional counting rules follows from the nominal scaling of the hard-scattering amplitude: $T_H \sim 1/Q^{n-4}$, where n is the total number of fields (quarks, leptons, or gauge fields) participating in the hard scattering [29, 39]. Thus the reaction is dominated by subprocesses and Fock states involving the minimum number of interacting fields. In the case of $2 \to 2$ scattering amplitudes, this implies $\frac{d\sigma}{dt}(AB \to CD) = F_{AB \to CD}(t/s)/s^{n-2}$. In the case of form factors, the dominant helicity conserving amplitude obeys $F(t) \sim (1/t)^{n_H - 1}$ where n_H is the minimum number of fields in the hadron H. The full predictions from PQCD modify the nominal scaling by logarithms from the running coupling and the evolution of the distribution amplitudes. In some cases, such as large angle $pp \to pp$ scattering, there can be "pinch" contributions [40] when the scattering can occur from a sequence of independent near-on shell quark-quark scattering amplitudes at the same CM angle. After inclu-

sion of Sudakov suppression form factors, these contributions also have a scaling behavior close to that predicted by constituent counting.

As shown by Maldacena [41], there is a remarkable correspondence between large N_C supergravity theory in a higher dimensional anti-de Sitter space and supersymmetric QCD in 4-dimensional space-time. String/gauge duality provides a framework for predicting QCD phenomena based on the conformal properties of the ADS/CFT correspondence. In a remarkable recent development, Polchinski and Strassler [42] have derived the dimensional counting rules using string duality, mapping features of gravitational theories in higher dimensions (AdS_5) to physical QCD in ordinary 3+1 space-time. The power-law fall-off of hard exclusive hadron-hadron scattering amplitudes at large momentum transfer can be derived without the use of perturbation theory by using the scaling properties of the hadronic interpolating fields in the large-r region of AdS space.

The distribution amplitudes which control leading-twist exclusive amplitudes at high momentum transfer can be related to the gauge-invariant Bethe-Salpeter wavefunction at equal light-cone time $\tau = x^+$. The logarithmic evolution of the hadron distribution amplitudes $\phi_H(x_i, Q)$ with respect to the resolution scale Q can be derived from the perturbatively-computable tail of the valence light-cone wavefunction in the high transverse momentum regime. The DGLAP evolution of quark and gluon distributions can also be derived in an analogous way by computing the variation of the Fock expansion with respect to the separation scale. Other key features of the perturbative QCD analyses are: (a) evolution equations for distribution amplitudes which incorporate the operator product expansion, renormalization group invariance, and conformal symmetry [38, 43, 44, 45, 46]; (b) hadron helicity conservation which follows from the underlying chiral structure of QCD [23]; (c) color transparency, which eliminates corrections to hard exclusive amplitudes from initial and final state interactions at leading power and reflects the underlying gauge theoretic basis for the strong interactions [47] and (d) hidden color degrees of freedom in nuclear wavefunctions, which reflect the color structure of hadron and nuclear wavefunctions [48]. There have also been recent advances eliminating renormalization scale ambiguities in hard-scattering amplitudes via commensurate scale relations [49] which connect the couplings entering exclusive amplitudes to the α_V coupling which controls the QCD heavy quark potential.

EXCLUSIVE TIMELIKE REACTIONS AND HADRON HELICITY CONSERVATION

Measurements of exclusive hadronic amplitudes in the timelike domain can test many basic principles of QCD, including factorization principles, dimensional counting rules, hadron helicity conservation, color transparency and

the possible role of higher Fock states such as intrinsic charm. Dimensional counting rules test the near conformal nature of QCD at moderate to high momentum transfers. The essential prediction for the production cross section of N hadrons each emitted at distinct fixed CM angles is the leading power-law prediction

$$\frac{dR_{e^+e^- \to H_1 H_2 \ldots H_N}}{d\Omega_1 d\Omega_2 \ldots d\Omega_{N-1}}(s) \propto \left[\frac{\alpha_s \Lambda_{QCD}^2}{s}\right]^{n_{tot}-2}, \quad (5)$$

where n_{tot} is the total number of quark and gluon constituents in the final state hadrons. The prediction is modified by possible anomalous dimensions and the running of the QCD coupling. However, there is now substantial theoretical and empirical evidence that the QCD coupling has an effective IR fixed point and can be treated as a constant over a large range of momentum transfers. In the case of two-body final states, this scaling predicts $s F_H(s) \to$ const for meson pairs and $s^2 F_H(s) \to$ const for baryon pairs, $s^5 F(s) \to$ const for deuteron pairs, and $s^4 F(s) \to$ const for pentaquark pairs. As discussed in the introduction, the anomalous fall-off of the proton to Δ transition form factor may indicate a dominance of higher Fock states in the Δ. This can be tested by measuring the power-law fall-off of $e^+ e^- \to \overline{p}\Delta$.

Hadron helicity conservation (HHC) is a QCD selection rule concerning the behavior of helicity amplitudes at high momentum transfer, such as fixed CM scattering. Since the convolution of T_H with the light-cone wavefunctions projects out states with $L_z = 0$, the leading hadron amplitudes conserve hadron helicity [23, 22]. Thus the dominant amplitudes are those in which the sum of hadron helicities in the initial state equals the sum of hadron helicities in the final state; other helicity amplitudes are relatively suppressed by an inverse power in the momentum transfer.

The study of time-like hadronic form factors using $e^+ e^-$ colliding beams can provide very sensitive tests of hadron helicity conservation, since the virtual photon in $e^+ e^- \to \gamma^* \to h_A \overline{h}_B$ always has spin ± 1 along the beam axis at high energies. Angular momentum conservation implies that the virtual photon can "decay" with one of only two possible angular distributions in the center of momentum frame: $(1 + \cos^2\theta)$ for $|\lambda_A - \lambda_B| = 1$ and $\sin^2\theta$ for $|\lambda_A - \lambda_B| = 0$ where λ_A and λ_B are the helicities of the outgoing hadrons. Hadronic helicity conservation, as required by QCD, greatly restricts the possibilities. It implies that $\lambda_A + \lambda_B = 0$. Consequently, angular momentum conservation requires $|\lambda_A| = |\lambda_B| = l/2$ for baryons, and $|\lambda_A| = |\lambda_B| = 0$ for mesons; thus the angular distributions for any sets of hadron pairs are now completely determined at leading twist: $\frac{d\sigma}{d\cos\theta}(e^+ e^- = B\overline{B}) \propto 1 + \cos^2\theta$ and $\frac{d\sigma}{d\cos\theta}(e^+ e^- = M\overline{M}) \propto \sin^2\theta$. Verifying these angular distributions for vector mesons and other higher spin mesons and baryons would verify the vector nature of the gluon in QCD and the validity of PQCD applications to exclusive reactions. In the case of vector pseudoscalar channels, parity conservation requires that the vector meson has $J_z = \pm 1$. Thus the vector-pseudoscalar meson pairs must

be suppressed in the leading twist limit; *e.g.*

$$\frac{\sigma_{e^+e^- \to \rho\pi}(s)}{\sigma_{e^+e^- \to \pi^+\pi^-}(s)} \propto \frac{\Lambda_{QCD}^2}{s} \ . \quad (6)$$

Surprisingly, this critical PQCD prediction has not been tested. If it fails, the perturbative QCD approach to hard exclusive hadron processes including the QCD factorization predictions for exclusive B decays would be in question.

In the case of electron-proton scattering, hadron helicity conservation states that the proton helicity-conserving form factor (which is proportional to G_M) dominates over the proton helicity-flip amplitude (proportional to $G_E/\sqrt{\tau}$) at large momentum transfer. Here $\tau = Q^2/4M^2, Q^2 = -q^2$. Thus HHC predicts $G_E(Q^2)/\sqrt{\tau}G_M(Q^2) \to 0$ at large Q^2. The new data from Jefferson Laboratory [50] which shows a decrease in the ratio $G_E(Q^2)/G_M(Q^2)$ is not itself in disagreement with the HHC prediction.

The leading-twist QCD motivated form $Q^4 G_M(Q^2) \simeq$ const$/Q^4 \ln Q^2 \Lambda^2$ provides a good guide to both the time-like and spacelike proton form factor data at $Q^2 > 5$ GeV^2 [51]. However, the Jefferson Laboratory data [50] appears to suggest $Q F_2(Q^2)/F_1(Q^2) \simeq$ const, for the ratio of the proton's Pauli and Dirac form factors in contrast to the nominal expectation $Q^2 F_2(Q^2)/F_1(Q^2) \simeq$ const expected (modulo logarithms) from PQCD. It should however be emphasized that a PQCD-motivated fit is not precluded. For example, the form

$$\frac{F_2(Q^2)}{F_1(Q^2)} = \frac{\mu_A}{1 + (Q^2/c)\ln^b(1 + Q^2/a)} \quad (7)$$

with $\mu_A = 1.79$, $a = 4m_\pi^2 = 0.073$ GeV^2, $b = -0.5922$, $c = 0.9599$ GeV^2 also fits the data well [52].

It is usually assumed that a heavy quarkonium state such as the J/ψ always decays to light hadrons via the annihilation of its heavy quark constituents to gluons. However, as Karliner and I [24] have shown, the transition $J/\psi \to \rho\pi$ can also occur by the rearrangement of the $c\overline{c}$ from the J/ψ into the $|q\overline{q}c\overline{c}\rangle$ intrinsic charm Fock state of the ρ or π. On the other hand, the overlap rearrangement integral in the decay $\psi' \to \rho\pi$ will be suppressed since the intrinsic charm Fock state radial wavefunction of the light hadrons will evidently not have nodes in its radial wavefunction. This observation provides a natural explanation of the long-standing puzzle why the J/ψ decays prominently to two-body pseudoscalar-vector final states in conflict with HHC, whereas the ψ' does not. If the intrinsic charm explanation is correct, then this mechanism will complicate the analysis of virtually all heavy hadron decays such as $J/\psi \to p\overline{p}$. In addition, the existence of intrinsic charm Fock states, even at a few percent level, provides new, competitive decay mechanisms for B decays which are nominally CKM-suppressed [53]. For example, the weak decays of the B-meson to two-body exclusive states consisting of strange plus light hadrons, such as $B \to \pi K$, are expected to be dominated by penguin contributions since the tree-level $b \to su\overline{u}$ decay is CKM suppressed. However, higher Fock

states in the B wave function containing charm quark pairs can mediate the decay via a CKM-favored $b \to s c \bar{c}$ tree-level transition. The presence of intrinsic charm in the b meson can be checked by the observation of final states containing three charmed quarks, such as $B \to J/\psi D \pi$ [54].

Figure 4: Process for measuring the timelike Compton amplitude $\gamma^* \to H \overline{H} \gamma$.

TIMELIKE VIRTUAL COMPTON SCATTERING

The Compton amplitude $\gamma \pi \to \gamma \pi$ is the simplest two-body scattering amplitude in QCD after lepton-meson scattering. Despite its fundamental importance, the meson Compton amplitude has never been measured directly. However, one can make interesting measurements of the timelike Compton amplitude using $e^+ e^- \to \gamma^* \to H \overline{H} \gamma$. See Fig. 4. More generally, one can use electron-positron annihilation to measure the timelike Compton amplitude for virtually any hadron: $\gamma^* \to H \overline{H} \gamma$ where H can be any neutral or charged meson or baryon. The interference with the radiative return amplitude $e^+ e^- \to e^+ e^- \gamma \to \gamma^* \gamma \to H \overline{H} \gamma$, which is proportional to the timelike form factor $F_H(q^2)$, can be measured through $H \leftrightarrow \overline{H}$ charge and single-spin asymmetries. One can also measure timelike transition Compton amplitudes $\gamma^* \to H \overline{H}^*$ and timelike form factors. In principle, the spacelike and timelike amplitudes are related by crossing and dispersion theory to generalized parton distributions; in practice, the timelike analysis involves even more complexities than virtual Compton scattering. One of the most interesting measures is the two-hadron distribution amplitude $\phi_{H\overline{H}}(x, \mathcal{M}^2, \widetilde{Q}^2)$ which measures the transition between a $q\bar{q}$ state and the $H \overline{H}$ hadron pair with invariant mass $\mathcal{M}^2 = (p_H + p_{\overline{H}})^2$ [55, 56]. One can factorize this distribution amplitude from the timelike virtual Compton amplitude when the quark propagator has high virtuality $\widetilde{Q}^2$. It obeys the same operator product expansion and the same type of logarithmic $\widetilde{Q}^2$ evolution as the pion distribution amplitude.

The $\gamma^* \gamma \to \pi^+ \pi^-$ hadron pair process is related to virtual Compton scattering on a pion target by crossing. The leading-twist amplitude is also sensitive to the $1/x - 1/(1 - x)$ moment of the two-pion distribution amplitude coupled to two valence quarks.

The virtual Compton scattering amplitudes $T(\gamma^* \to H \overline{H} \gamma)$ have extraordinary sensitivity to fundamental features of hadron structure [57, 58, 59, 60, 61, 62, 63, 64]. Even though the final-state photon is on-shell, the deeply virtual Compton process probes the elementary quark structure of the hadron near the light cone as an effective local current. In the spacelike case, the scaling, Regge behavior, and phase structure of deeply virtual Compton scattering $\gamma^* p \to \gamma p$ have been discussed in the context of the covariant parton model in Ref. [65]. The interference of Compton and bremsstrahlung amplitudes gives an electron-positron asymmetry in the $e^\pm p \to e^\pm \gamma p$ cross section which is proportional to the real part of the Comp-
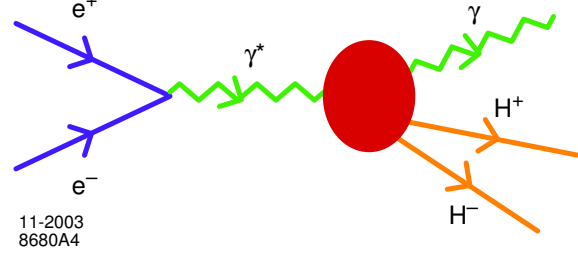
ton amplitude [65].

To leading order in $1/Q$, the deeply virtual Compton scattering amplitude $\gamma^* p \to \gamma p$ factorizes as the convolution in x of the amplitude $t^{\mu\nu}$ for hard Compton scattering on a quark line with the generalized Compton form factors $H(x, t, \zeta)$, $E(x, t, \zeta)$, $\widetilde{H}(x, t, \zeta)$, and $\widetilde{E}(x, t, \zeta)$ of the target proton. Here x is the light-cone momentum fraction of the struck quark, and $\zeta = Q^2/2P \cdot q$ plays the role of the Bjorken variable. The form factor $H(x, t, \zeta)$ describes the proton response when the helicity of the proton is unchanged, and $E(x, t, \zeta)$ is for the case when the proton helicity is flipped. Two additional functions $\widetilde{H}(x, t, \zeta)$, and $\widetilde{E}(x, t, \zeta)$ appear, corresponding to the dependence of the Compton amplitude on quark helicity. These "skewed" parton distributions involve non-zero momentum transfer, so that a probabilistic interpretation is not possible. However, there are remarkable sum rules connecting the chiral-conserving and chiral-flip form factors $H(x, t, \zeta)$ and $E(x, t, \zeta)$ with the corresponding spin-conserving and spin-flip electromagnetic form factors $F_1(t)$ and $F_2(t)$ and gravitational form factors $A_q(t)$ and $B_q(t)$ for each quark and anti-quark constituent [57]. Thus deeply virtual Compton scattering is related to the quark contribution to the form factors of a proton scattering in a gravitational field. All of these form factors can be measured for timelike photons in $\gamma^* \to H \overline{H} \gamma$ for protons as well as other hadrons.

CHARGE ASYMMETRIES IN TIMELIKE EXCLUSIVE REACTIONS

The discrepancy between the Rosenbluth and polarization transfer methods determinations of the proton form factors has led to a focus on the role of two-photon exchange amplitudes in $ep \to ep$ scattering. In the timelike case, the interference between the one- and two-photon exchange amplitudes in $e^+ e^- \to H \overline{H}$ leads to a charge asymmetry at order α a difference in the angular distribution of H vs. $\overline{H}$ relative to the incident electron direction. See Fig. 5. This angular asymmetry thus measures the relative phase of the $\gamma^* \gamma^* \to H \overline{H}$ timelike Compton amplitude and the timelike form factor $\gamma^* \to H \overline{H}$. One also has to take into account the contribution to the asymmetry

due to the interference of amplitudes from soft photon radiation from the lepton and hadron system. One can use the charge asymmetry in $e^+e^- \to \mu^+\mu^-$ as the standard.
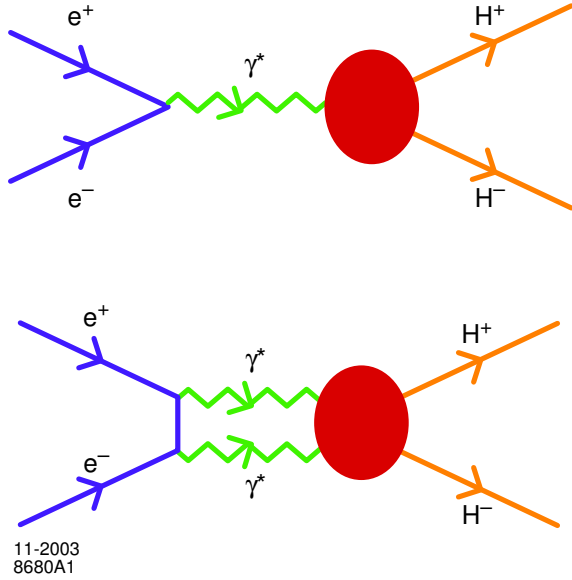

11-2003
8680A1

Figure 5: Interference of one and two-photon exchange amplitudes for $e^+e^- \to H\overline{H}$

The theory of the two-photon exchange amplitude involves all of the complexities of the doubly-virtual timelike Compton amplitude $\gamma^*\gamma^* \to H\overline{H}$. At high virtualities one expects a quark handbag approximation [37] to be valid. The hadron asymmetry will then mimic the corresponding $e^+e^- \to \mu^+\mu^-$ asymmetry weighted by the sum of quark charge squares and the $\langle \frac{1}{x} \rangle$ $j = 0$ moment characteristic of a $j = 0$ fixed pole in Regge theory [66]. A careful measurement of the charge asymmetry in charged meson and baryon pair production could illuminate the role of two-photon exchange in exclusive amplitudes.

THE PHOTON-TO-PION TRANSITION FORM FACTOR AND THE PION DISTRIBUTION AMPLITUDE

The simplest and perhaps most elegant illustration of an exclusive reaction in QCD is the evaluation of the photon-to-pion transition form factor $F_{\gamma \to \pi}(Q^2)$ which is measurable in single-tagged two-photon $ee \to ee\pi^0$ reactions. The form factor is defined via the invariant amplitude $\Gamma^\mu = -ie^2 F_{\pi\gamma}(Q^2)\epsilon^{\mu\nu\rho\sigma}p_\nu^\pi \epsilon_\rho q_\sigma$. As in inclusive reactions, one must specify a factorization scheme which divides the integration regions of the loop integrals into hard and soft momenta, compared to the resolution scale $\widetilde{Q}$. At leading twist, the transition form factor then factorizes as a convolution of the $\gamma^*\gamma \to q\bar{q}$ amplitude (where the quarks are collinear with the final state pion) with the

valence light-cone wavefunction of the pion:

$$F_{\gamma M}(Q^2) = \frac{4}{\sqrt{3}} \int_0^1 dx \phi_M(x, \widetilde{Q}) T_{\gamma \to M}^H(x, Q^2). \quad (8)$$

The hard scattering amplitude for $\gamma\gamma^* \to q\bar{q}$ is $T_{\gamma M}^H(x, Q^2) = [(1-x)Q^2]^{-1}(1 + \mathcal{O}(\alpha_s))$. The leading QCD corrections have been computed by Braaten [67]. The evaluation of the next-to-leading corrections in the physical α_V scheme is given in Ref. [68]. For the asymptotic distribution amplitude $\phi_\pi^{\text{asympt}}(x) = \sqrt{3}f_\pi x(1-x)$ one predicts $Q^2 F_{\gamma\pi}(Q^2) = 2f_\pi \left(1 - \frac{5}{3}\frac{\alpha_V(Q^*)}{\pi}\right)$ where $Q^* = e^{-3/2}Q$ is the BLM scale for the pion form factor. The PQCD predictions have been tested in measurements of $e\gamma \to e\pi^0$ by the CLEO collaboration [69]. The flat scaling of the $Q^2 F_{\gamma\pi}(Q^2)$ data from $Q^2 = 2$ to $Q^2 = 8$ GeV^2 provides an important confirmation of the applicability of leading twist QCD to this process. The magnitude of $Q^2 F_{\gamma\pi}(Q^2)$ is remarkably consistent with the predicted form, assuming the asymptotic distribution amplitude and including the LO QCD radiative correction with $\alpha_V(e^{-3/2}Q)/\pi \simeq 0.12$. One could allow for some broadening of the distribution amplitude with a corresponding increase in the value of α_V at small scales. Radyushkin [70], Ong [71] and Kroll [72] have also noted that the scaling and normalization of the photon-to-pion transition form factor tends to favor the asymptotic form for the pion distribution amplitude and rules out broader distributions such as the two-humped form suggested by QCD sum rules [73].

The photon-to-pion transition form factor $F_{\gamma \to \pi}(q^2)$ is the simplest hadronic matrix element in QCD and also one the most fundamental. As noted above, the matrix element $\langle \pi^0 | j^\mu(0) | \gamma \rangle$ transition form factor for spacelike momenta has been measured in the spacelike domain $q^2 < 0$ by scattering electrons on photons: $e\gamma \to e\pi^0$. However, $F_{\gamma \to \pi}(q^2)$ can also be measured in the timelike domain $q^2 = s > 0$ using $e^+e^-\gamma^* \to \pi^0\gamma$. See Fig. 6. Since the pion has positive C, there is no background from radiative return. Predictions for timelike q^2 van be made by analytic continuation. It would be very valuable to test the PQCD predictions in the timelike domain, including the effect of vector mesons in the approach to scaling. One also can test predictions for the $\gamma \to H^0$ form factor for any $C = +$ meson or hadronic system. A comprehensive discussion of the transition form factors for spacelike and timelike q^2 is given in Ref. [74].

EXCLUSIVE TWO-PHOTON ANNIHILATION INTO HADRON PAIRS

Two-photon reactions, $\gamma\gamma \to H\overline{H}$ at large s $= (k_1 + k_2)^2$ and fixed θ_{cm}, provide a particularly important laboratory for testing QCD since these cross-channel Compton processes are the simplest calculable large-angle exclusive hadronic scattering reactions involving two hadrons. See Fig. 7. The helicity structure, and often even the absolute normalization can be computed for the leading power-law contribution for each two-photon channel [75].
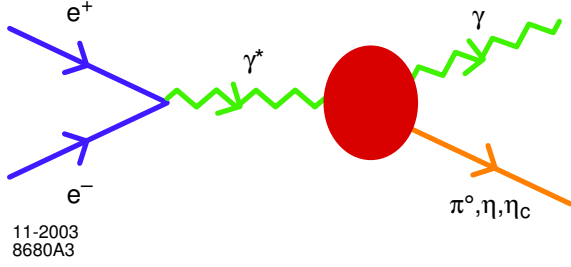
Figure 6: Process for measuring the timelike photon to meson transition amplitude $\gamma^* \to M_0\gamma$.

In the case of meson pairs, dimensional counting predicts that for large s, $s^4 d\sigma/dt(\gamma\gamma \to M\overline{M}$ scales at fixed t/s or $\theta_{\text{c.m.}}$ up to factors of $\ln s/\Lambda^2$.
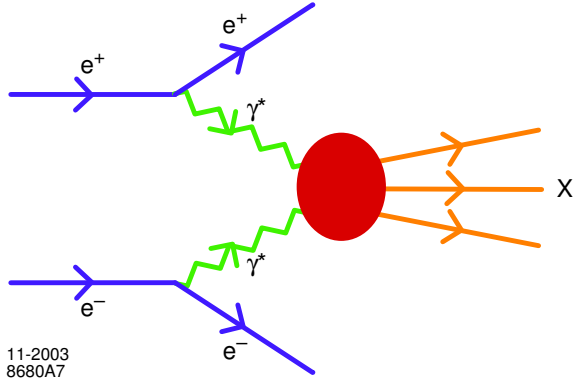

Figure 7: Illustration of two virtual photon annihilation in lepton-lepton collisions. The final state can be single $C = +$ hadrons, hadron pairs (double virtual Compton), or more general $C = +$ systems.

The angular dependence of the $\gamma\gamma \to H\overline{H}$ amplitudes can be used to determine the shape of the process-independent distribution amplitudes, $\phi_H(x, Q)$. An important feature of the $\gamma\gamma \to M\overline{M}$ amplitude for meson pairs is that the contributions of Landshoff pitch singularities are power-law suppressed at the Born level—even before taking into account Sudakov form factor suppression. There are also no anomalous contributions from the $x \to 1$ endpoint integration region. Thus, as in the calculation of the meson form factors, each fixed-angle helicity amplitude can be written to leading order in $1/Q$ in the factorized form $[Q^2 = p_T^2 = tu/s; \widetilde{Q}_x = \min(xQ, (l-x)Q)]$:

$$\mathcal{M}_{\gamma\gamma \to M\overline{M}} = \int_0^1 dx \int_0^1 dy \phi_{\overline{M}}(y, \widetilde{Q}_y) \quad (9)$$
$$\times T_H(x, y, s, \theta_{\text{c.m.}} \phi_M(x, \widetilde{Q}_x),$$

where T_H is the hard-scattering amplitude $\gamma\gamma \to (q\bar{q})(q\bar{q})$ for the production of the valence quarks collinear with each meson, and $\phi_M(x, \widetilde{Q})$ is the amplitude for finding the va-

lence q and $\bar{q}$ with light-cone fractions of the meson's momentum, integrated over transverse momenta $k_\perp < \widetilde{Q}$. The contribution of non-valence Fock states are power-law suppressed. Furthermore, the helicity-selection rules [23] of perturbative QCD predict that vector mesons are produced with opposite helicities to leading order in $1/Q$ and all orders in α_s. The dependence in x and y of several terms in $T_{\lambda, \lambda'}$ is quite similar to that appearing in the meson's electromagnetic form factor. Thus much of the dependence on $\phi_M(x, Q)$ can be eliminated by expressing it in terms of the meson form factor. In fact, the ratio of the $\gamma\gamma \to \pi^+\pi^-$ and $e^+e^- \to \mu^+\mu^-$ amplitudes at large s and fixed θ_{CM} is nearly insensitive to the running coupling and the shape of the pion distribution amplitude:

$$\frac{\frac{d\sigma}{dt}(\gamma\gamma \to \pi^+\pi^-)}{\frac{d\sigma}{dt}(\gamma\gamma \to \mu^+\mu^-)} \sim \frac{4|F_\pi(s)|^2}{1 - \cos^2\theta_{\text{c.m.}}}. \quad (10)$$

The comparison of the PQCD prediction for the sum of $\pi^+\pi^-$ plus K^+K^- channels with CLEO data [76] is shown in Fig. 8. The CLEO data for charged pion and kaon pairs show a clear transition to the scaling and angular distribution predicted by PQCD [75] for $W = \sqrt{s_{\gamma\gamma}} > 2$ GeV.

It is particularly important to measure the magnitude and angular dependence of the two-photon production of neutral pions and $\rho^+\rho^-$ cross sections in view of the strong sensitivity of these channels to the shape of meson distribution amplitudes.

Perturbative QCD predicts a strong suppression of the leading-twist cross section for $\gamma\gamma \to \pi^0\pi^0$ relative to the cross section for $\gamma\gamma \to \pi^+\pi^-$. This suppression is due to the negative interference between the amplitudes involving two-quark currents with the single quark current amplitudes. This cancellation does not appear in models based on the handbag approximation [37] in which the only diagram which appears is a factorized on-shell $\gamma\gamma \to q\bar{q}$ Born amplitude. Thus the measurements of this ratio is crucial for testing the perturbative QCD factorization of exclusive amplitudes. A similar test can be carried out by measuring the neutral to charged pion pair ratio in $e^+e^- \to \pi\pi\gamma$.

QCD also predicts that the production cross section for charged ρ-pairs (with any helicity) is much larger that for that of neutral ρ pairs, particularly at large $\theta_{\text{c.m.}}$ angles. Similar predictions are possible for other helicity-zero mesons.

Baryon pair production in two-photon annihilation is also an important testing ground for QCD. The only available data is the cross channel reaction, $\gamma p \to \gamma p$. The calculation of T_H for Compton scattering requires the evaluation of 368 helicity-conserving tree diagrams which contribute to $\gamma(qqq) \to \gamma'(qqq)'$ at the Born level and a careful integration over singular intermediate energy denominators [77, 78, 59]. Brooks and Dixon [79] have recently completed a recalculation of the Compton process at leading order in PQCD, extending and correcting earlier work. It is useful to consider the ratio $s^6 d\sigma/dt(\gamma p \to \gamma p)/t^4 F_1^2(ep \to ep)$ where $F_1(t)$ is the
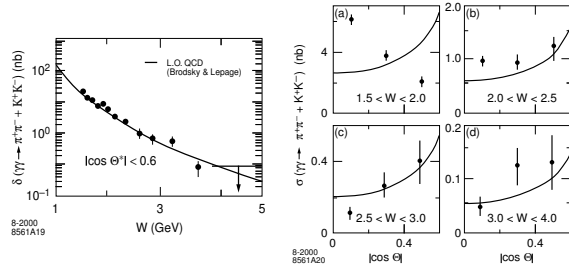
Figure 8: Comparison of the sum of $\gamma\gamma \to \pi^+\pi^-$ and $\gamma\gamma \to K^+K^-$ meson pair production cross sections with the scaling and angular distribution of the perturbative QCD prediction [75]. The data are from the CLEO collaboration [76].

elastic helicity-conserving Dirac form factor since the power-law fall-off, the normalization of the valence wavefunctions, and much of the uncertainty from the scale of the QCD coupling cancel. The scaling and angular dependence of this ratio is sensitive to the shape of the proton distribution amplitudes and appears to be consistent with the distribution amplitudes motivated by QCD sum rules. The normalization of the ratio at leading order is not predicted correctly by perturbative QCD. However, it is conceivable that the QCD loop corrections to the hard scattering amplitude are significantly larger than those of the elastic form factors in view of the much greater number of Feynman diagrams contributing to the Compton amplitude relative to the proton form factor. The perturbative QCD predictions for the phase of the Compton amplitude phase can be tested in virtual Compton scattering by interference with Bethe-Heitler processes [80].

Berger and Schweiger [81] have recently studied baryon pair production in two-photon collisions using perturbative QCD factorization treating baryons as quark-diquark systems. Their approach give a consistent description of the cross sections for all octet baryon channels, including most recent large-momentum-transfer data from LEP for the $\gamma\gamma \to \Lambda\overline{\Lambda}$. These prediction need to be compared with the standard QCD analysis based on the three quark structure of the baryons.

A debate has continued [82, 83, 84, 85] on whether processes such as the pion and proton form factors and elastic Compton scattering $\gamma p \to \gamma p$ might be dominated by higher-twist mechanisms until very large momentum transfer. If one assumes that the light-cone wavefunction of the pion has the form $\psi_{\text{soft}}(x, k_\perp) = A \exp(-b\frac{k_\perp^2}{x(1-x)})$, then the Feynman endpoint contribution to the overlap integral at small $k_\perp$ and $x \simeq 1$ will dominate the form factor compared to the hard-scattering contribution until very large Q^2. However, this ansatz for $\psi_{\text{soft}}(x, k_\perp)$ has no suppression at $k_\perp = 0$ for any x; *i.e.*, the wavefunction in the hadron rest frame does not fall-off at all for $k_\perp = 0$ and $k_z \to -\infty$. Thus such wavefunctions do not represent well soft QCD contributions. Endpoint contributions

are also suppressed by the QCD Sudakov form factor, reflecting the fact that a near-on-shell quark must radiate if it absorbs large momentum. One can show [38] that the leading power dependence of the two-particle light-cone Fock wavefunction in the endpoint region is $1 - x$, giving a meson structure function which falls as $(1 - x)^2$ and thus by duality a non-leading contribution to the meson form factor $F(Q^2) \propto 1/Q^3$. Thus the dominant contribution to meson form factors comes from the hard-scattering regime.

THE DOUBLY-VIRTUAL TIMELIKE COMPTON AMPLITUDE

One can measure the virtual Compton amplitude $T(\gamma_1^*\gamma_2^* \to H\overline{H})$ as a function of spacelike q_1^2, q_2^2 and $s \geq 4m_H^2$ in the two-photon reaction:

$$e^+e^- \to e^+e^-\gamma_1^*\gamma_2^* \to e^+e^-H\overline{H}. \tag{11}$$

This should be a possible measurement at high luminosity e^+e^- colliders, particularly for meson pairs.

Assuming that quark Compton scattering is dominant (and the $j = 0$ mechanism is relevant), we can predict the ratio of the leading power-law contribution to the virtual Compton amplitude at large q_1^2 and q_2^2 to the corresponding lepton pair production amplitude

$$\begin{aligned} R_{2\gamma}^{p\overline{p}}(q_1^2, q_2^2, s) &= \frac{T(\gamma_1^*\gamma_2^* \to H\overline{H})}{T(\gamma_1^*\gamma_2^* \to \mu^-\mu^+)} \\ &= (e_u^2 + e_d^2)\langle\frac{1}{x_q}\rangle F_H(s). \tag{12} \end{aligned}$$

The $C = +$ form factor $F_p(s)$ should be similar to the proton's timelike Dirac form factor $F_1(s)$.

Thus one can empirically check the theoretical assumptions underlying the two-photon exchange amplitude which we need to describe the radiative correction to elastic ep scattering. It is also an important constraint on the timelike $s \geq 4M_H^2$ input to the two-photon exchange amplitude which interferes with the one-photon amplitude to give the charge asymmetry in $e^+e^- \to H\overline{H}$.

PERTURBATIVE QCD CALCULATION OF BARYON FORM FACTORS

The baryon form factor at large momentum transfer provides an important example of the application of perturbative QCD to exclusive processes. Away from possible special points in the x_i integrations (which are suppressed by Sudakov form factors) baryon form factors can be written to leading order in $1/Q^2$ as a convolution of a connected hard-scattering amplitude T_H convoluted with the baryon distribution amplitudes. The Q^2-evolution of the baryon distribution amplitude can be derived from the operator product expansion of three quark fields or from the gluon exchange kernel. Taking into account the evolution of the baryon distribution amplitude, the nucleon magnetic

form factors at large Q^2, has the form [38, 86, 23]

$$G_M(Q^2) \rightarrow \frac{\alpha_s^2(Q^2)}{Q^4} \sum_{n,m} b_{nm} \left(\log \frac{Q^2}{\Lambda^2} \right)^{\gamma_n^B + \gamma_n^B}$$

$$\times \quad \left[1 + \mathcal{O} \left(\alpha_s(Q^2), \frac{m^2}{Q^2} \right) \right] \quad . \quad (13)$$

where the γ_n^B are computable anomalous dimensions [87] of the baryon three-quark wave function at short distance, and the b_{mn} are determined from the value of the distribution amplitude $\phi_B(x, Q_0^2)$ at a given point Q_0^2 and the normalization of T_H. Asymptotically, the dominant term has the minimum anomalous dimension. The contribution from the endpoint regions of integration, $x \sim 1$ and $y \sim 1$, at finite $k_\perp$ is Sudakov suppressed [30, 86, 38]; however, the endpoint region may play a significant role in phenomenology.

The proton form factor appears to scale at $Q^2 > 5$ GeV^2 according to the PQCD predictions. Nucleon form factors are approximately described phenomenologically by the well-known dipole form $G_M(Q^2) \simeq 1/(1 + Q^2/0.71 \text{ GeV}^2)^2$ which behaves asymptotically as $G_M(Q^2) \simeq (1/Q^4)(1 - 1.42 \text{ GeV}^2/Q^2 + \cdots)$. This suggests that the corrections to leading twist in the proton form factor and similar exclusive processes involving protons become important in the range $Q^2 < 1.4$ GeV^2.

Measurements for the timelike proton form factor using $\bar{p}p \to e^+e^-$ annihilation are reported in Ref. [7]. The results are consistent with perturbative QCD scaling. The ratio of the timelike to spacelike form factor depends in detail on the analytic continuation of the QCD coupling, anomalous dimensions [68].

The shape of the distribution amplitude controls the normalization of the leading-twist prediction for the proton form factor. If one assumes that the proton distribution amplitude has the asymptotic form: $\phi_N = C x_1 x_2 x_3$, then the convolution with the leading order form for T_H gives zero! If one takes a non-relativistic form peaked at $x_i = 1/3$, the sign is negative, requiring a crossing point zero in the form factor at some finite Q^2. The broad asymmetric distribution amplitudes advocated by Chernyak and Zhitnitsky [88, 89] gives a more satisfactory result. If one assumes a constant value of $\alpha_s = 0.3$, and $f_N = 5.3 \times 10^{-3}$GeV^2, the leading order prediction is below the data by a factor of ≈ 3. However, since the form factor is proportional to $\alpha_s^2 f_N^2$, one can obtain agreement with experiment by a simple renormalization of the parameters. For example, if one uses the central value [90] $f_N = 8 \times 10^{-3}$GeV^2, then good agreement is obtained [91]. The normalization of the proton's distribution amplitude is also important for determining the proton's lifetime [92, 93].

A useful technique for obtaining the solutions to the baryon evolution equations is to construct completely antisymmetric representations as a polynomial orthonormal basis for the distribution amplitude of multi-quark bound states. In this way one obtain a distinctive classification of

nucleon (N) and Delta (Δ) wave functions and the corresponding Q^2 dependence which discriminates N and Δ form factors. More recently Braun and collaborators have shown how one can use conformal symmetry to classify the eigensolutions of the baryon distribution amplitude [46]. They identify a new 'hidden' quantum number which distinguishes components in the $\lambda = 3/2$ distribution amplitudes with different scale dependence. They are able to find analytic solution of the evolution equation for $\lambda = 3/2$ and $\lambda = 1/2$ baryons where the two lowest anomalous dimensions for the $\lambda = 1/2$ operators (one for each parity) are separated from the rest of the spectrum by a finite 'mass gap'. These special states can be interpreted as baryons with scalar diquarks. Their results may support Carlson's solution [94] to the puzzle that the proton to Δ form factor falls faster [21] than other $p \to N^*$ amplitudes if the Δ distribution amplitude has a symmetric $x_1 x_2 x_3$ form.

SINGLE-SPIN POLARIZATION EFFECTS AND THE DETERMINATION OF TIMELIKE PROTON FORM FACTORS

Although the spacelike form factors of a stable hadron are real, the timelike form factors have a phase structure reflecting the final-state interactions of the outgoing hadrons. In general, form factors are analytic functions $F_i(q^2)$ with a discontinuity for timelike momentum above the physical threshold $q^2 > 4M^2$. The analytic structure and phases of the form factors in the timelike regime are thus connected by dispersion relations to the spacelike regime [95, 96, 97]. The analytic form and phases of the timelike amplitudes also reflects resonances in the unphysical region $0 < q^2 < 4M^2$ below the physical threshold [95] in the $J^{PC} = 1^{--}$ channel, including gluonium states and di-baryon structures.

Any model which fits the spacelike form factor data with an analytic function can be continued to the timelike region. Spacelike form factors are usually written in terms of $Q^2 = -q^2$. The correct relation for analytic continuation can be obtained by examining denominators in loop calculations in perturbation theory. The connection is $Q^2 \to q^2 e^{-i\pi}$, or

$$\ln Q^2 = \ln(-q^2) \to \ln q^2 - i\pi \ . \quad (14)$$

If the spacelike F_2/F_1 is fit by a rational function of Q^2, then the form factors will be relatively real in the timelike region also. However, one in general gets a complex result from the continuation.

At very large center-of-mass energies, perturbative QCD factorization predicts diminished final interactions in $e^+e^- \to H\bar{H}$, since the hadrons are initially produced with small color dipole moments. This principle of QCD color transparency [98] is also an essential feature [99] of hard exclusive B decays [100, 101], and it needs to be tested experimentally.

There have been a number of explanations and theoretically motivated fits of the new Jefferson laboratory F_2/F_1

data. Belitsky, Ji, and Yuan [102] have shown that factors of $\log(Q^2)$ arise from a careful QCD analysis of the form factors. The perturbative QCD form $Q^2 F_2/F_1 \sim \log^2 Q^2$, which has logarithmic factors multiplying the nominal power-law behavior, fits the large-Q^2 spacelike data well. Others [103, 104] claim to find mechanisms that modify the traditionally expected power-law behavior with fractional powers of Q^2, and they also give fits which are in accord with the data. Asymptotic behaviors of the ratio F_2/F_1 for general light-front wave functions are investigated in [52]. Each of the model forms predicts a specific fall-off and phase structure of the form factors from $s \leftrightarrow t$ crossing to the timelike domain. A fit with the dipole polynomial or nominal dimensional counting rule behavior would predict no phases in the timelike regime.

TIMELIKE MEASURES

The center-of-mass angular distribution provides the analog of the Rosenbluth method for measuring the magnitudes of various helicity amplitudes. The differential cross section for $e^- e^+ \rightarrow B\overline{B}$ when B is a spin-1/2 baryon is given in the center-of-mass frame by

$$\frac{d\sigma}{d\Omega} = \frac{\alpha^2 \beta}{4q^2} D , \qquad (15)$$

where $\beta = \sqrt{1 - 4m_B^2/q^2}$ and D is given by

$$D = |G_M|^2 \left(1 + \cos^2\theta\right) + \frac{1}{\tau} |G_E|^2 \sin^2\theta ; \qquad (16)$$

we have used the Sachs form factors [26]

$$\begin{aligned} G_M &= F_1 + F_2 , \\ G_E &= F_1 + \tau F_2 , \end{aligned} \qquad (17)$$

with $\tau \equiv q^2/4m_B^2 > 1$.

As noted by Dubnickova, Dubnicka, and Rekalo, and by Rock [105], the existence of the $T-$odd single-spin asymmetry normal to the scattering plane in baryon pair production $e^- e^+ \rightarrow B\overline{B}$ requires a nonzero phase difference between the G_E and G_M form factors. The phase of the ratio of form factors G_E/G_M of spin-1/2 baryons in the timelike region can thus be determined from measurements of the polarization of one of the produced baryons. In a recent paper, Carlson, Hiller, and Hwang and I have shown that measurements of the proton polarization in $e^+ e^- \rightarrow p\overline{p}$ strongly discriminate between the analytic forms of models which have been suggested to fit the proton G_E/G_M data in the spacelike region. Polarization observables can be used to completely pin down the relative phases of the timelike form factors. The complex phases of the form factors in the timelike region make it possible for a single outgoing baryon to be polarized in $e^- e^+ \rightarrow B\overline{B}$, even without polarization in the initial state.

There are three polarization observables, corresponding to polarizations in three directions denoted z, x, and y, respectively. Longitudinal polarization (z) refers to the polarization state parallel to the direction of the outgoing baryon.

Sideways (x) means perpendicular to the direction of the outgoing baryon but in the scattering plane. Normal (y) means normal to the scattering plane, in the direction of $\vec{k} \times \vec{p}$ where $\vec{k}$ is the electron momentum and $\vec{p}$ is the baryon momentum, with x, y, and z forming a right-handed coordinate system.

The polarization $\mathcal{P}_y$ does not require polarization in the initial state and is [105]

$$\mathcal{P}_y = \frac{\sin 2\theta \, \mathrm{Im} G_E^* G_M}{D\sqrt{\tau}} = \frac{(\tau - 1)\sin 2\theta \, \mathrm{Im} F_2^* F_1}{D\sqrt{\tau}} . \qquad (18)$$

The other two polarizations require initial state polarization. If the electron has polarization P_e then [105]

$$\mathcal{P}_x = -P_e \frac{2\sin\theta \, \mathrm{Re} G_E^* G_M}{D\sqrt{\tau}} , \qquad (19)$$

and

$$\mathcal{P}_z = P_e \frac{2\cos\theta |G_M|^2}{D} . \qquad (20)$$

The sign of $\mathcal{P}_z$ can be determined from physical principles. Angular momentum conservation and helicity conservation for the electron and positron determine that $\mathcal{P}_z/P_e$ in the forward direction must be $+1$, verifying the sign of the above formula.

The polarization measurement in $e^+ e^- \rightarrow p\overline{p}$ will require a polarimeter for the outgoing protons, perhaps based on a shell of a material such as carbon which has a good analyzing power. However, timelike baryon-antibaryon production can occur for any pair that is energetically allowed. Baryons such as the Σ and Λ which decay weakly are easier to study, since their polarization is self-analyzing.

The polarization $\mathcal{P}_y$ is a manifestation of the T-odd observable $\vec{k} \times \vec{p} \cdot \vec{S}_p$, with $\vec{S}_p$ the proton polarization. This observable is zero in the spacelike case, but need not be zero in the timelike case because final state interactions can give the form factors a relative phase.

One can also predict [106] the single-spin asymmetry $\mathcal{P}_y$ for QED processes such as $e^+ e^- \rightarrow \tau^+ \tau^-$ which is sensitive to the imaginary part of the timelike Schwinger correction to the lepton anomalous moment and Pauli form factor.

Predictions for polarization $\mathcal{P}_y$ in various models are shown in Fig. 9. The predicted polarizations are significant and are distinct from a purely polynomial fit to the spacelike data, which gives zero $\mathcal{P}_y$.

The predictions for $\mathcal{P}_x$ and $\mathcal{P}_z$ are shown in Figs. 10 and 11. Both figures are for scattering angle $45°$ and $P_e = 1$. The phase difference $(\delta_E - \delta_M)$ between G_E and G_M is directly given by the $\mathcal{P}_y/\mathcal{P}_x$ ratio,

$$\frac{\mathcal{P}_y}{\mathcal{P}_x} = \frac{\cos\theta}{P_e} \frac{\mathrm{Im} \, G_M^* G_E}{\mathrm{Re} \, G_M^* G_E} = \frac{\cos\theta}{P_e} \tan(\delta_E - \delta_M) . \qquad (21)$$

The magnetic form factor in the IJL model [107] is very small in the 10 to 20 GeV^2 region (taking the dipole form for comparison) and has a zero in the complex plane near $q^2 = 15$ GeV^2. This accounts for much of the different
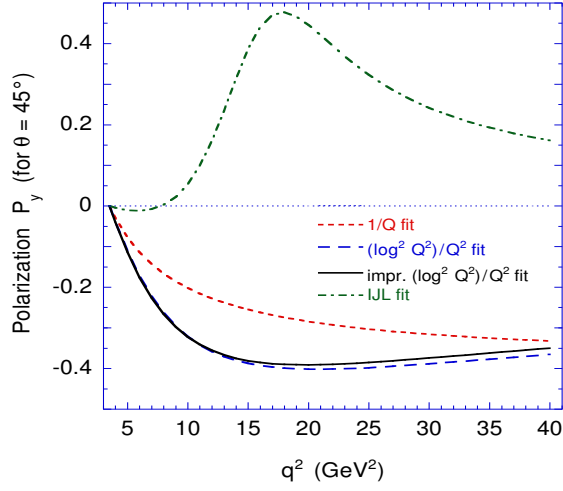
Figure 9: Predicted polarization $\mathcal{P}_y$ in the timelike region for selected form factor fits described in the text. The plot is for $\theta = 45°$. The four curves are for an $F_2/F_1 \propto 1/Q$ fit; the $(\log^2 Q^2)/Q^2$ fit of Belitsky et al.; an improved $(\log^2 Q^2)/Q^2$ fit; and a fit from Iachello et al. Details are given in Ref. [31].
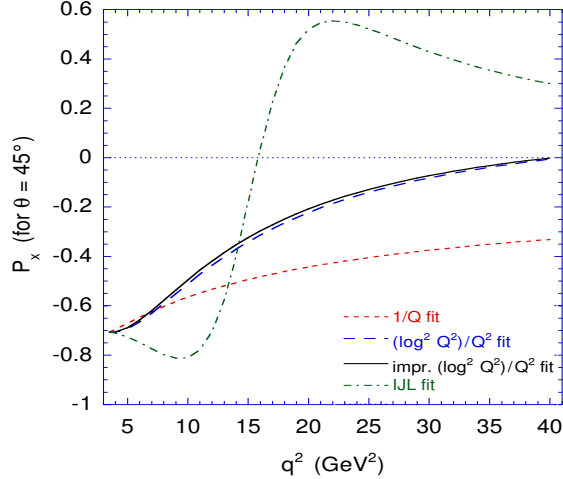

Figure 11: The predicted polarization $\mathcal{P}_z$ in the timelike region for $\theta = 45°$ and $P_e = 1$. The four curves correspond to those in Fig. 9.

Figure 10: The predicted polarization $\mathcal{P}_x$ in the timelike region for $\theta = 45°$ and $P_e = 1$. The four curves correspond to those in Fig. 9.

Figure 12: The predicted differential cross section $\sigma(\theta) \equiv d\sigma/d\Omega$. The four curves correspond to those in Fig. 9.

behavior of the IJL model seen in the polarization plots. The IJL ratio for G_E/G_M is large compared to the other three models, and this strongly affects the angular behavior of the differential cross section as shown in Fig. 12 for $q^2 = 10\,\text{GeV}^2$.

INCLUSIVE SINGLE-SPIN ASYMMETRIES

Spin correlations provide a remarkably sensitive window to hadronic structure and basic mechanisms in QCD.
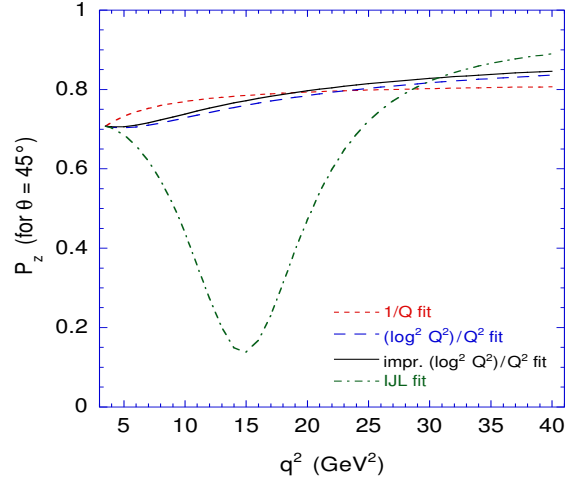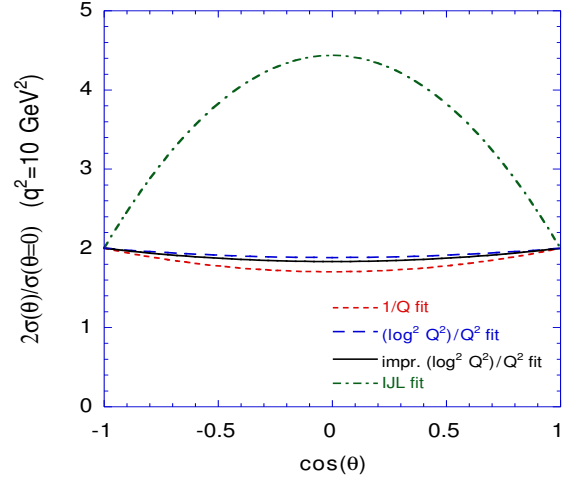
Among the most interesting polarization effects are single-spin azimuthal asymmetries (SSAs) in semi-inclusive deep inelastic scattering, representing the correlation of the spin of the proton target and the virtual photon to hadron production plane: $\vec{S}_p \cdot \vec{q} \times \vec{p}_H$ [108]. Such asymmetries are time-reversal odd, but they can arise in QCD through phase differences in different spin amplitudes.

The most common explanation of the pion electroproduction asymmetries in semi-inclusive deep inelastic scattering is that they are related to the transversity distribution of the quarks in the hadron h_1 [109, 110, 111] convoluted with the transverse momentum dependent fragmentation function $H_1^\perp$, the Collins function, which gives the distribution for a transversely polarized quark to fragment into an unpolarized hadron with non-zero transverse mo-

mentum [112, 113, 114, 115, 116].

The QCD final-state interactions (gluon exchange) between the struck quark and the proton spectators in semi-inclusive deep inelastic lepton scattering can produce Sivers-type single-spin asymmetries which survive in the Bjorken limit [117, 118, 119]. The fragmentation of the quark into hadrons is not necessary, and one has a correlation with the production plane of the quark jet itself $\vec{S}_p \cdot \vec{q} \times \vec{p}_q$. The required matrix element measures the spin-orbit correlation $\vec{S} \cdot \vec{L}$ within the target hadron's wave function, the same matrix element which produces the anomalous magnetic moment of the proton, the Pauli form factor, and the generalized parton distribution E which is measured in deeply virtual Compton scattering. Since the same matrix element controls the Pauli form factor, the contribution of each quark current to the SSA is proportional to the contribution $\kappa_{q/p}$ of that quark to the proton target's anomalous magnetic moment $\kappa_p = \sum_q e_q \kappa_{q/p}$ [117]. Avakian [108] has shown that the data from HERMES and Jefferson laboratory could be accounted for by the above analysis. However, more analyses and measurements, especially azimuthal angular correlations, will be needed to unambiguously separate the transversity and Sivers effect mechanisms.

Physically, the final-state interaction phase arises as the infrared-finite difference of QCD Coulomb phases for hadron wave functions with differing orbital angular momentum. The final-state interaction effects can be identified with the gauge link which is present in the gauge-invariant definition of parton distributions [118]. When the light-cone gauge is chosen, a transverse gauge link is required. Thus in any gauge the parton amplitudes need to be augmented by an additional eikonal factor incorporating the final-state interaction and its phase [119, 120]. The net effect is that it is possible to define transverse momentum dependent parton distribution functions which contain the effect of the QCD final-state interactions. The same final-state interactions are responsible for the diffractive component to deep inelastic scattering, and that they play a critical role in nuclear shadowing phenomena [121].

Measurements from Jefferson Lab [122] also show significant beam single spin asymmetries in deep inelastic scattering. Afanasev and Carlson [123] have recently shown that this asymmetry is due to the interference of longitudinal and transverse photoabsorption amplitudes which have different phases induced by the final-state interaction between the struck quark and the target spectators just as in the calculations of Ref. [117]. Their results are consistent with the experimentally observed magnitude of this effect. Thus similar FSI mechanisms involving quark orbital angular momentum appear to be responsible for both target and beam single-spin asymmetries.

A related analysis shows that the initial-state interactions from gluon exchange between the incoming quark and the target spectator system will lead to leading-twist single-spin target spin asymmetries in the Drell-Yan process $H_1 H_2 \to \ell^+ \ell^- X$ [124, 125]. Initial-state interac-

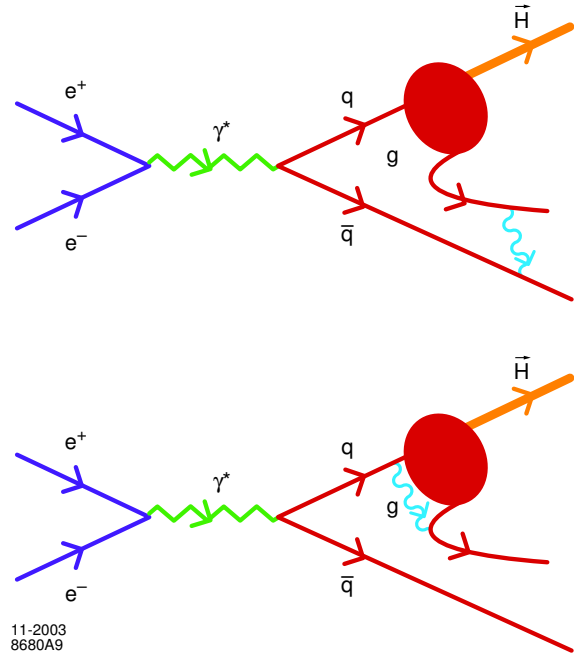tions also lead to a $\cos 2\phi$ planar correlation in unpolarized Drell-Yan reactions [126].

Figure 13: Illustration of the final-state gluon exchange which produces single-spin asymmetries in inclusive electron-positron collisions.

We can also consider the SSA of $e^+ e^-$ annihilation processes for any inclusive process producing a polarizable hadron, such as $e^+ e^- \to \gamma^* \to \pi \Lambda X$. The Λ reveals its polarization via its decay $\Lambda \to p \pi^-$. The final state gluon exchange mechanism which causes $T - odd$ spin correlations in inclusive $e^+ e^-$ annihilation processes is illustrated in Fig. 13. The spin of the Λ is normal to the decay plane. Thus we can look for a SSA through the T-odd correlation $\epsilon_{\mu\nu\rho\sigma} S_\Lambda^\mu p_\Lambda^\nu q_{\gamma^*}^\rho p_\pi^\sigma$. This is related by crossing to SIDIS on a Λ target. In addition one can consider single spin asymmetries in inclusive reactions such as $e^+ e^- \to \gamma^* \to \pi X$ involving the incident polarized electron beam.

TESTING SOFT PION THEOREMS IN THE TIMELIKE DOMAIN

In an important theoretical development, Pobylitsa *et al.* [127] have shown how to compute transition form factors linking the proton to nucleon-pion states which have minimal invariant mass W. A new soft pion theorem for high momentum transfers allows one to compute the three-quark distribution amplitudes for the near threshold pion states from a chiral rotation. The new soft pion results are in a good agreement with the SLAC electroproduction data for $W^2 < 1.4 \text{ GeV}^2$ and $7 < Q^2 < 30.7 \text{ GeV}^2$.

The soft pion analysis can be applied to timelike reactions such as $e^+ e^- \to p \bar{n} \pi^+$ in the regime where the pion is emitted at small relative rapidity with respect to one of

the outgoing nucleons. The fall-off of the cross sections should be identical to that of $e^+e^- \to p\bar{p}$.

NEAR-THRESHOLD COULOMB CORRECTIONS

One of the most interesting effects due to QED radiative corrections is the Coulomb correction to production of charges pairs near threshold. The lowest order Coulomb exchange is illustrated in Fig. 14. The original theory is due to Sommerfeld. For example,

$$\sigma(e^+e^- \to \bar{p}p) = \sigma_0(e^+e^- \to \bar{p}p)\frac{X}{1-\exp{-X}} \quad (22)$$

where $\frac{X=\pi\alpha}{\beta}$, with $\beta^2 = 1 - \frac{4M_p^2}{s}$. Thus the absolute square of measured timelike form factors $|G_M^p|^2$ and $|G_E^p|^2$ are corrected by the factor $\frac{X}{1-\exp{-X}} \sim \frac{\pi\alpha}{\beta}$ for small velocities $\beta \ll \pi\alpha$. Thus the Coulomb correction becomes infinite at zero relative velocity $\beta \to 0$! The Coulomb-corrected cross section is finite at threshold, although the Born cross section vanishes linearly with β due to the vanishing phase space. Observation of the angular distribution of τ pair production can provide a measurement of the magnetic moment of the τ [128].

11-2003
8680A2

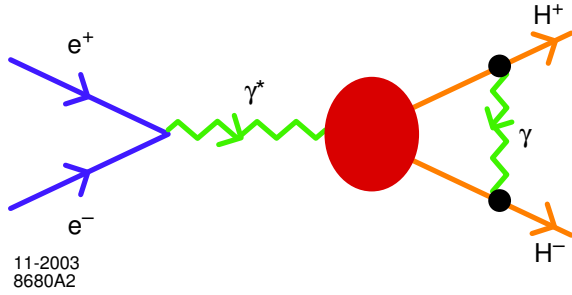Figure 14: Final state Coulomb correction to charged hadron pair production

The Coulomb enhancement in $e^+e^- \to H^+H^-$ is dual to the presence of Coulomb H^+H^- bound states just below threshold. In the case of $e^+e^- \to \mu^+\mu^-$ and $e^+e^- \to \tau^+\tau^-$ there is an accumulation of Bohr levels from "true muonium" ($\mu^+\mu^-$) and "true tauonium" ($\tau^+\tau^-$) just below the continuum.

It would be interesting to observe these Coulomb bound-state atoms. In the case of $(p\bar{p})$, $(\pi^+\pi^-)$, (D^+D^-), etc., the $S-wave$ Coulomb states decay hadronically via annihilation, but the nonzero orbital states could be quasi-stable. It is possible that the threshold enhancements seen in $p\bar{p} \to e^+e^-$, and $J/\psi \to \gamma p\bar{p}$ is due to the Coulomb enhancements.

QCD THRESHOLD EFFECTS

One can expect strong effects analogous to the QED Coulomb effects whenever heavy quarks are produced at low relative velocity with respect to each other or with other quarks. The opening of the strangeness and charm threshold in timelike e^+e^- and $\gamma\gamma$ reactions show sensitivity to this physics. Two distinctly different scales arise as arguments of the QCD coupling near threshold: the relative momentum of the quarks governing the soft gluon exchange responsible for the Coulomb potential, and a large momentum scale approximately equal to twice the quark mass for the corrections induced by transverse gluons. One can use the angular Distribution of heavy quarks to obtains a direct determination of the heavy quark potential. Predictions for the angular distribution of massive quarks and leptons are presented in Ref. [128], including the fermionic part of the two-loop corrections to the electromagnetic form factors using with the BLM scale-fixing prescription.

EFFECTIVE QCD CHARGES AND CONFORMAL ASPECTS OF QCD

One can define the coupling α_s of QCD from virtually any physical observable [129, 130]. Such couplings, called effective charges, are all-order resummations of perturbation theory, so they correspond to the complete theory of QCD; it is thus guaranteed that they are analytic and non-singular. An important example is the effective charge α_R where $1 + \frac{\alpha_R(s)}{\pi}$ is defined from the ratio of the total e^+e^- annihilation cross section to the leading order QCD prediction. Unlike the $\overline{\text{MS}}$ coupling, a physical coupling is analytic across quark flavor thresholds [131, 132]. Furthermore, a physical coupling must stay finite in the infrared when the momentum scale goes to zero. In turn, this means that integrals over the running coupling are well defined for physical couplings. Once such a physical coupling $\alpha_{\text{phys}}(k^2)$ is chosen, other physical quantities can be expressed as expansions in α_{phys} by eliminating the $\overline{\text{MS}}$ coupling which now becomes only an intermediary [49]. In such a procedure there are in principle no further renormalization scale (μ) or scheme ambiguities. The physical couplings satisfy the standard renormalization group equation for its logarithmic derivative, $d\alpha_{\text{phys}}/d\ln k^2 = \widehat{\beta}_{\text{phys}}[\alpha_{\text{phys}}(k^2)]$, where the first two terms in the perturbative expansion of the Gell-Mann Low function $\widehat{\beta}_{\text{phys}}$ are scheme-independent at leading twist, whereas the higher order terms have to be calculated for each observable separately using perturbation theory.

The effective charge $\alpha_\tau(s)$ can be defined using the high precision measurements of the hadronic decay channels of the $\tau^- \to \nu_\tau h^-$. Let R_τ be the ratio of the hadronic decay rate to the leptonic one. Then $R_\tau \equiv R_\tau^0 \left[1 + \frac{\alpha_\tau}{\pi}\right]$, where R_τ^0 is the zeroth order QCD prediction, defines the effective charge α_τ. The data for τ decays is well-understood channel by channel, thus allowing the calculation of the hadronic decay rate and the effective charge as a function of the τ mass below the physical mass [133]. The vector and axial-vector decay modes which can be studied separately.

Using an analysis of the τ data from the OPAL collaboration [134], we have found that the experimental value of the coupling $\alpha_\tau(s) = 0.621 \pm 0.008$ at $s = m_\tau^2$ corresponds to a value of $\alpha_{\overline{MS}}(M_Z^2) = (0.117\text{-}0.122) \pm 0.002$, where the range corresponds to three different perturbative methods used in analyzing the data. This result is in good agreement with the world average $\alpha_{\overline{MS}}(M_Z^2) = 0.117 \pm 0.002$. However, from the figure we also see that the effective charge only reaches $\alpha_\tau(s) \sim 0.9 \pm 0.1$ at $s = 1\,\text{GeV}^2$, and it even stays within the same range down to $s \sim 0.5\,\text{GeV}^2$.

The results for $\alpha_\tau(s)$ are in good agreement with the estimate of Mattingly and Stevenson [135] for the effective coupling $\alpha_R(s) \sim 0.85$ for $\sqrt{s} < 0.3\,\text{GeV}$ determined from e^+e^- annihilation, especially if one takes into account the perturbative commensurate scale relation, $\alpha_\tau(m_{\tau'}^2) = \alpha_R(s^*)$ where, for $\alpha_R = 0.85$, we have $s^* \simeq 0.10\,m_{\tau'}^2$. This behavior is not consistent with the coupling having a Landau pole, but rather shows that the physical coupling is close to constant at low scales, suggesting that physical QCD couplings are effectively constant or "frozen" at low scales. It is important to carefully extend the analysis of α_R using annihilation data of higher precision and energy.

Figure 15 compares the experimentally determined effective charge $\alpha_\tau(s)$ with solutions to the evolution equation for α_τ at two-, three-, and four-loop order normalized at m_τ. At three loops the behavior of the perturbative solution drastically changes, and instead of diverging, it freezes to a value $\alpha_\tau \simeq 2$ in the infrared. The reason for this fundamental change is, the negative sign of $\beta_{\tau,2}$. This result is not perturbatively stable since the evolution of the coupling is governed by the highest order term. This is illustrated by the widely different results obtained for three different values of the unknown four loop term $\beta_{\tau,3}$ which are also shown[1] It is interesting to note that the central four-loop solution is in good agreement with the data all the way down to $s \simeq 1\,\text{GeV}^2$.

It has also been argued that $\alpha_R(s)$ freezes perturbatively to all orders [137]. In fact since all observables are related by commensurate scale relations, they all should have an IR fixed point [138]. This result is also consistent with Dyson-Schwinger equation studies of the physical gluon propagator in Landau gauge [139, 140].

The near constancy of the effective QCD coupling at small scales helps explain the empirical success of dimensional counting rules for the power law fall-off of form factors and fixed angle scaling. One can calculate the hard scattering amplitude T_H for such processes [38] without scale ambiguity in terms of the effective charge α_τ or α_R using commensurate scale relations [68, 141]. The effective coupling is evaluated in the regime where the coupling is approximately constant, in contrast to the rapidly varying behavior from powers of α_s predicted by perturbation theory (the universal two-loop coupling). For ex-
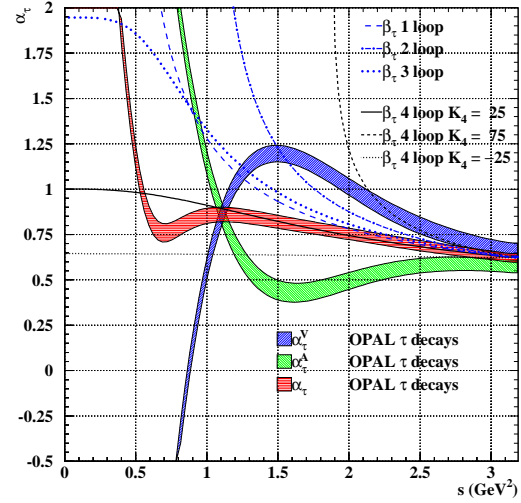

Figure 15: The effective charge α_τ for non-strange hadronic decays of a hypothetical τ lepton with $m_{\tau'}^2 = s$ compared to solutions of the fixed order evolution equation for α_τ at two-, three-, and four-loop order. The error bands include statistical and systematic errors.

ample, the nucleon form factors are proportional at leading order to two powers of α_s evaluated at low scales in addition to two powers of $1/q^2$; The pion photoproduction amplitude at fixed angles is proportional at leading order to three powers of the QCD coupling. The essential variation from leading-twist counting-rule behavior then only arises from the anomalous dimensions of the hadron distribution amplitudes. The magnitude of the effective charge [68] $\alpha_s^{\text{exclusive}}(Q^2) = F_\pi(Q^2)/4\pi Q^2 F_{\gamma\pi^0}^2(Q^2)$ for exclusive amplitudes is connected to α_τ by a commensurate scale relation. Its magnitude: $\alpha_s^{\text{exclusive}}(Q^2) \sim 0.8$ at small Q^2, is sufficiently large as to explain the observed magnitude of exclusive amplitudes such as the pion form factor.

There are a number of useful phenomenological consequences of near conformal behavior: the conformal approximation with zero β function can be used as template for QCD analyses [142, 143] such as the form of the expansion polynomials for distribution amplitudes [46]. The near-conformal behavior of QCD is also the basis for commensurate scale relations [49] which relate observables to each other without renormalization scale or scheme ambiguities [144]. In this method the effective charges of observables are related to each other in conformal gauge theory; the effects of the nonzero QCD $\beta-$ function are then taken into account using the BLM method [145] to set the scales of the respective couplings. An important example is the generalized Crewther relation [146] which allow one to calculate unambiguously without renormalization scale or scheme ambiguity the effective charges of the polarized Bjorken and the Gross-Llewellen Smith sum rules from the experimental value for the effective charge associated

with $R_{e^+e^-}(s)$. Present data are consistent with the generalized Crewther relations within errors, but measurements at higher precision in e^+e^- annihilation are needed to decisively test these fundamental relations in QCD. Such measurements are also crucial for a high precision evaluation of the hadronic corrections to the muon anomalous magnetic moment [147]. The discrepancy between the annihilation cross section in the isospin $I = 1$ channel and the corresponding isospin $I = 1$ data from τ decay also needs to be resolved [148].

ACKNOWLEDGEMENTS

REFERENCES

[1] K. Abe *et al.* [Belle Collaboration], Phys. Rev. Lett. **89**, 142001 (2002) [arXiv:hep-ex/0205104].

[2] For a review and references, see B. L. Ioffe and D. E. Kharzeev, arXiv:hep-ph/0306062.

[3] S. J. Brodsky, A. S. Goldhaber and J. Lee, Phys. Rev. Lett. **91**, 112001 (2003) [arXiv:hep-ph/0305269].

[4]

[4] J. Z. Bai *et al.* [BES Collaboration], Phys. Rev. Lett. **91**, 022001 (2003) [arXiv:hep-ex/0303006].

[5] K. Abe *et al.* [Belle Collaboration], Phys. Rev. Lett. **88**, 181803 (2002) [arXiv:hep-ex/0202017].

[6] K. Abe *et al.* [Belle Collaboration], Phys. Rev. Lett. **89**, 151802 (2002) [arXiv:hep-ex/0205083].

[7] M. Andreotti *et al.*, Phys. Lett. B **559**, 20 (2003).

[8] S. J. Brodsky, I. A. Schmidt and G. F. de Teramond, Phys. Rev. Lett. **64**, 1011 (1990).

[9] M. E. Luke, A. V. Manohar and M. J. Savage, Phys. Lett. B **288**, 355 (1992) [arXiv:hep-ph/9204219].

[10] J. M. Richard, Nucl. Phys. Proc. Suppl. **86**, 361 (2000) [arXiv:nucl-th/9909030].

[11] A. Datta and P. J. O'Donnell, Phys. Lett. B **567**, 273 (2003) [arXiv:hep-ph/0306097].

[12] T. Nakano *et al.* [LEPS Collaboration], Phys. Rev. Lett. **91**, 012002 (2003) [arXiv:hep-ex/0301020].

[13] V. V. Barmin *et al.* [DIANA Collaboration], Phys. Atom. Nucl. **66**, 1715 (2003) [Yad. Fiz. **66**, 1763 (2003)] [arXiv:hep-ex/0304040].

[14] S. Stepanyan *et al.* [CLAS Collaboration], arXiv:hep-ex/0307018.

[15] J. Barth *et al.* [SAPHIR Collaboration], arXiv:hep-ex/0307083.

[16] D. Diakonov, V. Petrov and M. V. Polyakov, Z. Phys. A **359**, 305 (1997) [arXiv:hep-ph/9703373].

[17] F. Close, arXiv:hep-ph/0311087.

[18] M. Karliner and H. J. Lipkin, arXiv:hep-ph/0307243.

[19] D. P. Roy, arXiv:hep-ph/0311207.

[20] C. E. Carlson, C. D. Carone, H. J. Kwee and V. Nazaryan, Phys. Lett. B **573**, 101 (2003) [arXiv:hep-ph/0307396].

[21] P. Stoler, Phys. Rept. **226**, 103 (1993).

[22] V. Chernyak, [arXiv:hep-ph/9906387].

[23] S. J. Brodsky and G. P. Lepage, Phys. Rev. **D24**, 2848 (1981).

[24] S. J. Brodsky and M. Karliner, Phys. Rev. Lett. **78**, 4682 (1997), hep-ph/9704379.

[25] M. K. Jones *et al.* [Jefferson Lab Hall A Collaboration], Phys. Rev. Lett. **84**, 1398 (2000). O. Gayou *et al.* [Jefferson Lab Hall A Collaboration], Phys. Rev. Lett. **88**, 092301 (2002).

[26] R. G. Sachs, Phys. Rev. **126**, 2256 (1962); J. D. Walecka, Nuovo Cim. **11**, 821 (1959).

[27] P. A. Guichon and M. Vanderhaeghen, hep-ph/0306007; P. G. Blunden, W. Melnitchouk, and J. A. Tjon, nucl-th/0306076.

[28] R. G. Arnold, C. E. Carlson, and F. Gross, Phys. Rev. C **23**, 363 (1981), and other references cited therein.

[29] S. J. Brodsky and G. R. Farrar, Phys. Rev. D **11**, 1309 (1975); V. A. Matveev, R. M. Muradian, and A. N. Tavkhelidze, Lett. Nuovo Cim. **7** (1973) 719.

[30] G. P. Lepage and S. J. Brodsky, Phys. Rev. Lett. **43**, 545 (1979).

[31] S. J. Brodsky, C. E. Carlson, J. R. Hiller and D. S. Hwang, arXiv:hep-ph/0310277.

[32] A. Aloisio *et al.* [KLOE Collaboration], arXiv:hep-ex/0107023.

[33] E. P. Solodov [BABAR collaboration], in *Proc. of the e^+e^- Physics at Intermediate Energies Conference* ed. Diego Bettoni, eConf **C010430**, T03 (2001) [arXiv:hep-ex/0107027].

[34] B. Aubert *et al.* [BABAR Collaboration], arXiv:hep-ex/0310027.

[35] S. J. Brodsky, C. E. Carlson and R. Suaya, Phys. Rev. D **14**, 2264 (1976).

[36] S. J. Brodsky, J. F. Gunion and R. L. Jaffe, Phys. Rev. D **6**, 2487 (1972).

[37] See P. Kroll, arXiv:hep-ph/0310327, and references therein.

[38] G. P. Lepage and S. J. Brodsky, Phys. Rev. D **22**, 2157 (1980).

[39] V. A. Matveev, R. M. Muradian and A. N. Tavkhelidze, Lett. Nuovo Cim. **7**, 719 (1973).

[40] P. V. Landshoff, Phys. Rev. D **10**, 1024 (1974).

[41] J. M. Maldacena, Adv. Theor. Math. Phys. **2**, 231 (1998) [Int. J. Theor. Phys. **38**, 1113 (1999)] [arXiv:hep-th/9711200].

[42] J. Polchinski and M. J. Strassler, Phys. Rev. Lett. **88**, 031601 (2002) [arXiv:hep-th/0109174].

[43] S. J. Brodsky, Y. Frishman, G. P. Lepage and C. Sachrajda, Phys. Lett. **91B**, 239 (1980).

[44] D. Muller, Phys. Rev. D **51**, 3855 (1995) [arXiv:hep-ph/9411338].

[45] P. Ball and V. M. Braun, Nucl. Phys. B **543**, 201 (1999) [arXiv:hep-ph/9810475].

[46] V. M. Braun, S. E. Derkachov, G. P. Korchemsky and A. N. Manashov, Nucl. Phys. **B553**, 355 (1999) [arXiv:hep-ph/9902375].

[47] S. J. Brodsky and A. H. Mueller, Phys. Lett. **B206**, 685 (1988).

[48] S. J. Brodsky, C. R. Ji and G. P. Lepage, Phys. Rev. Lett. **51**, 83 (1983).

[49] S. J. Brodsky and H. J. Lu, Phys. Rev. D **51**, 3652 (1995) [arXiv:hep-ph/9405218].

[50] M. K. Jones [Jefferson Lab Hall A Collaboration], Nucl. Phys. A **699**, 124 (2002). O. Gayou *et al.* [Jefferson Lab Hall A Collaboration], Phys. Rev. Lett. **88**, 092301 (2002) [arXiv:nucl-ex/0111010]. Phys. Rev. Lett. **84**, 1398 (2000) [arXiv:nucl-ex/9910005].

[51] M. Ambrogiani *et al.* [E835 Collaboration], Phys. Rev. D **60**, 032002 (1999).

[52] S. J. Brodsky, J. R. Hiller, D. S. Hwang, and V. A. Karmanov, hep-ph/0311218.

[53] S. J. Brodsky and S. Gardner, Phys. Rev. D **65**, 054016 (2002) [arXiv:hep-ph/0108121].

[54] C. H. Chang and W. S. Hou, Phys. Rev. D **64**, 071501 (2001).

[55] D. Muller, D. Robaschik, B. Geyer, F. M. Dittes, and J. Horejsi, Fortsch. Phys. **42**, 101 (1994), hep-ph/9812448.

[56] M. Diehl, T. Gousset, and B. Pire, [arXiv:hep-ph/0003233].

[57] Ji, X., Talk presented at 12th Int. Symp. on High-Energy Spin Physics (SPIN96), Amsterdam, Sep. 1996, hep-ph/9610369; *Phys. Rev. Lett.* **78** (1997) 610; Ji, X., Phys. Rev. **D55**, 7114 (1997), hep-ph/9609381. Ji, X., J. Phys. **G 24**, 1181 (1998), hep-ph/9807358; Ji, X. and Osborne, J., Phys. Rev. **D 58**, 094018 (1998), hep-ph/9801260.

[58] A. V. Radyushkin, Phys. Rev. **D56**, 5524 (1997) [hep-ph/9704207].

[59] P. A. Guichon and M. Vanderhaeghen, Prog. Part. Nucl. Phys. **41**, 125 (1998) [arXiv:hep-ph/9806305].

[60] M. Vanderhaeghen, P. A. Guichon, and M. Guidal, Phys. Rev. Lett. **80**, 5064 (1998).

[61] J. C. Collins and A. Freund, Phys. Rev. **D 59**, 074009 (1999), hep-ph/9801262.

[62] M. Diehl, T. Feldmann, R. Jakob, and P. Kroll, Phys. Lett. **B460**, 204 (1999) hep-ph/9903268; Diehl, M., Feldmann, T., Jakob, R. and Kroll, P., Eur. Phys. J. **C8**, 409 (1999), hep-ph/9811253.

[63] J. Blumlein and D. Robaschik, hep-ph/0002071.

[64] M. Penttinen, M. V. Polyakov, A. G. Shuvaev, and M. Strikman, hep-ph/0006321.

[65] S. J. Brodsky, F. E. Close, and J. F. Gunion, Phys. Rev. **D 5**, 1384 (1972); Phys. Rev. **D 6**, 177 (1972); Phys. Rev. **D 8**, 3678 (1973).

[66] A. Afanasev, S. J. Brodsky, and C. E. Carlson, (in preparation).

[67] E. Braaten and S.-M. Tse, Phys. Rev. **D35**, 2255 (1987).

[68] S. J. Brodsky, C. R. Ji, A. Pang and D. G. Robertson, Phys. Rev. D **57**, 245 (1998) [arXiv:hep-ph/9705221].

[69] J. Gronberg *et al.* [CLEO Collaboration], Phys. Rev. **D57**, 33 (1998), hep-ex/9707031.

[70] A. V. Radyushkin, Acta Phys. Polon. **B26**, 2067 (1995).

[71] S. Ong, Phys. Rev. **D52**, 3111 (1995).

[72] P. Kroll and M. Raulfs, Phys. Lett. **387B**, 848 (1996).

[73] V. L. Chernyak and A. R. Zhitnitsky, Phys. Rep. **112**, 173 (1984).

[74] D. Melikhov, O. Nachtmann, V. Nikonov and T. Paulus, arXiv:hep-ph/0311213.

[75] S. J. Brodsky and G. P. Lepage, Phys. Rev. **D24**, 1808 (1981).

[76] H. Paar *et al.*, CLEO collaboration (to be published). V. Savinov, in *Proc. of the e^+e^- Physics at Intermediate Energies Conference* ed. Diego Bettoni, eConf **C010430**, W03 (2001) [arXiv:hep-ex/0106013]. See also D. Morgan, M. R. Pennington and M. R. Whalley, DPDG-94-01. H. Aihara *et al.* [TPC/Two Gamma Collaboration], Phys. Rev. D **40** (1989) 2772. K. Grzelak [DELPHI Collaboration], Nucl. Phys. Proc. Suppl. **82**, 316 (2000).

[77] G. R. Farrar, and H. Zhang, Phys. Rev. Lett. **65**, 1721 (1990).

[78] A. S. Kronfeld and B. Nizic, Phys. Rev. **D44**, 3445 (1991).

[79] T. C. Brooks and L. J. Dixon, Phys. Rev. D **62**, 114021 (2000) [arXiv:hep-ph/0004143].

[80] S. J. Brodsky, F. E. Close and J. F. Gunion, Phys. Rev. **D6**, 177 (1972).

[81] C. F. Berger and W. Schweiger, Eur. Phys. J. C **28**, 249 (2003) [arXiv:hep-ph/0212066].

[82] N. Isgur and C. H. Llewellyn Smith, Phys. Lett. **B217**, 535 (1989).

[83] A. V. Radyushkin, Phys. Rev. **D58**, 114008 (1998), hep-ph/9803316.

[84] J. Bolz and P. Kroll, Z. Phys. **A356**, 327 (1996), hep-ph/9603289.

[85] M. Diehl, P. Kroll and C. Vogt, Eur. Phys. J. C **22**, 439 (2001) [arXiv:hep-ph/0108220].

[86] G. P. Lepage and S. J. Brodsky, Phys. Lett. **B 87**, 359 (1979).

[87] M. E. Peskin, Phys. Lett. **B88**, 128 (1979).

[88] V. L. Chernyak and I. R. Zhitnitsky, Nucl. Phys. **B246**, 52 (1984).

[89] V. L. Chernyak, A. A. Ogloblin and I. R. Zhitnitsky, Z. Phys. **C42**, 583 (1989).

[90] V. M. Belyaev and B. L. Ioffe, Sov. Phys. JETP **56**, 493 (1982) [Zh. Eksp. Teor. Fiz. **83**, 876 (1982)].

[91] N. G. Stefanis, Eur. Phys. J. **C7**, 1 (1999) [arXiv:hep-ph/9911375].

[92] V. S. Berezinsky, B. L. Ioffe and Y. I. Kogan, Phys. Lett. B **105**, 33 (1981).

[93] S. J. Brodsky, J. R. Ellis, J. S. Hagelin and C. T. Sachrajda, Nucl. Phys. B **238**, 561 (1984).

[94] C. E. Carlson, Phys. Rev. **D34**, 2704 (1986).

[95] R. Baldini, E. Pasqualucci, S. Dubnicka, P. Gauzzi, S. Pacetti and Y. Srivastava, Nucl. Phys. A **666**, 38 (2000); R. Baldini, S. Dubnicka, P. Gauzzi, S. Pacetti, E. Pasqualucci, and Y. Srivastava, Eur. Phys. J. C **11**, 709 (1999).

[96] For a discussion on the validity of continuing spacelike form factors to the timelike region, see, B. V. Geshkenbein, B. .L. Ioffe, and M. A. Shifman, Sov. J. Nucl. Phys. **20**, 66 (1975) [Yad. Fiz. **20**, 128 (1974)]; R. Baldini, E. Pasqualucci, S. Dubnicka, P. Gauzzi, S. Pacetti and Y. Srivastava, in *Proc. of the e^+e^- Physics at Intermediate Energies Conference* ed. Diego Bettoni, eConf **C010430**, T20 (2001) [arXiv:hep-ph/0106006].

[97] See also R. Calabrese, in *Proc. of the e^+e^- Physics at Intermediate Energies Conference* ed. Diego Bettoni, eConf **C010430**, W07 (2001); R. Baldini-Ferroli, E. Pasqualucci, C. Bini and P. Patteri, Form-Factors," Nucl. Phys. Proc. Suppl. **56**, 275 (1997); H. W. Hammer, *ibid.*, W08 (2001) [arXiv:hep-ph/0105337]; A. Antonelli *et al.* [FENICE Collaboration], *Prepared for International Conference on Physics with GeV Particle Beams, Julich, Germany, 22-25 Aug 1994* Carl E. Carlson, *ibid.*, W09 (2001) [arXiv:hep-ph/0106290]; M. Karliner, *ibid.*, W10 (2001) [arXiv:hep-ph/0108106].

[98] S. J. Brodsky and A. H. Mueller, Phys. Lett. B **206**, 685 (1988).

[99] J. D. Bjorken, Nucl. Phys. Proc. Suppl. **11**, 325 (1989).

[100] M. Beneke, G. Buchalla, M. Neubert and C. T. Sachrajda, Nucl. Phys. B **606**, 245 (2001) [arXiv:hep-ph/0104110].

[101] Y. Y. Keum, H. N. Li and A. I. Sanda, Phys. Rev. D **63**, 054008 (2001) [arXiv:hep-ph/0004173].

[102] A. V. Belitsky, X. Ji, and F. Yuan, Phys. Rev. Lett. **91**, 092003 (2003). arXiv:hep-ph/0212351.

[103] J. P. Ralston and P. Jain, hep-ph/0302043; J. P. Ralston, P. Jain, and R. V. Buniy, AIP Conf. Proc. **549**, 302 (2000) [hep-ph/0206074].

[104] G. A. Miller and M. R. Frank, Phys. Rev. C **65**, 065205 (2002); [arXiv:nucl-th/0201021]; M. R. Frank, B. K. Jennings, and G. A. Miller, Phys. Rev. C **54**, 920 (1996). [arXiv:nucl-th/9509030].

[105] A. Z. Dubnickova, S. Dubnicka, and M. P. Rekalo, Nuovo Cim. A **109**, 241 (1996); S. Rock, *Proc. of the e^+e^- Physics at Intermediate Energies Conference* ed. Diego Bettoni, eConf **C010430**, W14 (2001) [hep-ex/0106084].

[106] S. J. Brodsky and D. S. Hwang, to be published.

[107] F. Iachello, A. D. Jackson, and A. Lande, Phys. Lett. B **43**, 191 (1973).

[108] H. Avakian [CLAS Collaboration], *Workshop on Testing QCD through Spin Observables in Nuclear Targets, Charlottesville, Virginia, 18-20 Apr 2002*

[109] R.L. Jaffe, hep-ph/9602236.

[110] D. Boer, Nucl. Phys. Proc. Suppl. **105**, 76 (2002) [hep-ph/0109221].

[111] D. Boer, Nucl. Phys. **A 711**, 21 (2002) [hep-ph/0206235].

[112] J. C. Collins, Nucl. Phys. **B 396**, 161 (1993).

[113] V. Barone, A. Drago and P.G. Ratcliffe, Phys. Rept. **359**, 1 (2002).

[114] B. Q. Ma, I. Schmidt and J. J. Yang, Phys. Rev. D **66**, 094001 (2002) [arXiv:hep-ph/0209114].

[115] G. R. Goldstein and L. Gamberg, arXiv:hep-ph/0209085.

[116] L. P. Gamberg, G. R. Goldstein and K. A. Oganessyan, Phys. Rev. D **67**, 071504 (2003) [arXiv:hep-ph/0301018].

[117] S. J. Brodsky, D. S. Hwang and I. Schmidt, Phys. Lett. B **530**, 99 (2002) [arXiv:hep-ph/0201296].

[118] J.C. Collins, Phys. Lett. **B 536**, 43 (2002).

[119] X. Ji and F. Yuan, Phys. Lett. **B 543**, 66 (2002).

[120] A. V. Belitsky, X. Ji and F. Yuan, Nucl. Phys. B **656**, 165 (2003) [arXiv:hep-ph/0208038].

[121] S. J. Brodsky, P. Hoyer, N. Marchal, S. Peigne and F. Sannino, Phys. Rev. D **65**, 114025 (2002) [arXiv:hep-ph/0104291].

[122] H. Avakian *et al.* [CLAS Collaboration], arXiv:hep-ex/0301005.

[123] A. Afanasev and C. E. Carlson, arXiv:hep-ph/0308163.

[124] J. C. Collins, Phys. Lett. B **536**, 43 (2002) [arXiv:hep-ph/0204004].

[125] S.J. Brodsky, D.S. Hwang and I. Schmidt, Nucl. Phys. **B 642**, 344 (2002).

[126] D. Boer, S. J. Brodsky and D. S. Hwang, Phys. Rev. D **67**, 054003 (2003) [arXiv:hep-ph/0211110].

[127] P. V. Pobylitsa, V. Polyakov and M. Strikman, Phys. Rev. Lett. **87**, 022001 (2001) [arXiv:hep-ph/0101279].

[128] S. J. Brodsky, A. H. Hoang, J. H. Kuhn and T. Teubner, Phys. Lett. B **359**, 355 (1995) [arXiv:hep-ph/9508274].

[129] G. Grunberg, Phys. Lett. **B95**, 70 (1980) [Erratum-ibid. **B110**, 501 (1982)].

[130] G. Grunberg, Phys. Rev. **D29**, 2315 (1984).

[131] S. J. Brodsky, M. S. Gill, M. Melles and J. Rathsman, Phys. Rev. D **58**, 116006 (1998) [arXiv:hep-ph/9801330].

[132] S. J. Brodsky, M. Melles and J. Rathsman, Phys. Rev. D **60**, 096006 (1999) [arXiv:hep-ph/9906324].

[133] S. J. Brodsky, S. Menke, C. Merino and J. Rathsman, Phys. Rev. D **67**, 055008 (2003) [arXiv:hep-ph/0212078].

[134] K. Ackerstaff *et al.* [OPAL Collaboration], Eur. Phys. J. C **7**, 571 (1999) [arXiv:hep-ex/9808019].

[135] A. C. Mattingly and P. M. Stevenson, Phys. Rev. D **49**, 437 (1994) [arXiv:hep-ph/9307266].

[136] F. Le Diberder and A. Pich, Phys. Lett. **B289**, 165 (1992).

[137] D. M. Howe and C. J. Maxwell, Phys. Lett. B **541**, 129 (2002) [arXiv:hep-ph/0204036].

[138] D. M. Howe and C. J. Maxwell, arXiv:hep-ph/0303163.

[139] L. von Smekal, R. Alkofer and A. Hauck, Phys. Rev. Lett. **79**, 3591 (1997) [arXiv:hep-ph/9705242].

[140] D. Zwanziger, arXiv:hep-ph/0303028.

[141] B. Melic, B. Nizic and K. Passek, Phys. Rev. D **65**, 053020 (2002) [arXiv:hep-ph/0107295].

[142] S. J. Brodsky, Y. Frishman and G. P. Lepage, Phys. Lett. B **167**, 347 (1986).

[143] S. J. Brodsky, P. Damgaard, Y. Frishman and G. P. Lepage, Phys. Rev. D **33**, 1881 (1986).

[144] S. J. Brodsky, E. Gardi, G. Grunberg and J. Rathsman, Phys. Rev. D **63**, 094017 (2001) [arXiv:hep-ph/0002065].

[145] S. J. Brodsky, G. P. Lepage and P. B. Mackenzie, Phys. Rev. D **28**, 228 (1983).

[146] S. J. Brodsky, G. T. Gabadadze, A. L. Kataev and H. J. Lu, Phys. Lett. **B372**, 133 (1996) [arXiv:hep-ph/9512367].

[147] M. Davier, S. Eidelman, A. Hocker and Z. Zhang, arXiv:hep-ph/0308213.

[148] S. Ghozzi and F. Jegerlehner, arXiv:hep-ph/0310181.